

# The Interconversion of UDP-Arabinopyranose and UDP-Arabinofuranose Is Indispensable for Plant Development in *Arabidopsis*

Carsten Rautengarten,<sup>a</sup> Berit Ebert,<sup>a</sup> Thomas Herter,<sup>b</sup> Christopher J. Petzold,<sup>c</sup> Tadashi Ishii,<sup>d</sup> Aindrita Mukhopadhyay,<sup>c</sup> Björn Usadel,<sup>b</sup> and Henrik Vibe Scheller<sup>a,e,1</sup>

<sup>a</sup> Joint BioEnergy Institute, Feedstocks Division, Lawrence Berkeley National Laboratory, Emeryville, California 94608

<sup>b</sup> Max-Planck-Institute of Molecular Plant Physiology, 14476 Golm, Germany

<sup>c</sup> Joint BioEnergy Institute, Technology Division, Lawrence Berkeley National Laboratory, Emeryville, California 94608

<sup>d</sup> Forestry and Forest Products Research Institute, Tsukuba, Ibaraki 305-8687, Japan

<sup>e</sup> Department of Plant and Microbial Biology, University of California, Berkeley, California 94720

**L-Ara, an important constituent of plant cell walls, is found predominantly in the furanose rather than in the thermodynamically more stable pyranose form. Nucleotide sugar mutases have been demonstrated to interconvert UDP-L-arabinopyranose (UDP-Arap) and UDP-L-arabinofuranose (UDP-Araf) in rice (*Oryza sativa*). These enzymes belong to a small gene family encoding the previously named Reversibly Glycosylated Proteins (RGPs). RGPs are plant-specific cytosolic proteins that tend to associate with the endomembrane system. In *Arabidopsis thaliana*, the RGP protein family consists of five closely related members. We characterized all five RGPs regarding their expression pattern and subcellular localizations in transgenic *Arabidopsis* plants. Enzymatic activity assays of recombinant proteins expressed in *Escherichia coli* identified three of the *Arabidopsis* RGP protein family members as UDP-L-Ara mutases that catalyze the formation of UDP-Araf from UDP-Arap. Coimmunoprecipitation and subsequent liquid chromatography-electrospray ionization-tandem mass spectrometry analysis revealed a distinct interaction network between RGPs in different *Arabidopsis* organs. Examination of cell wall polysaccharide preparations from *RGP1* and *RGP2* knockout mutants showed a significant reduction in total L-Ara content (12–31%) compared with wild-type plants. Concomitant downregulation of *RGP1* and *RGP2* expression results in plants almost completely deficient in cell wall-derived L-Ara and exhibiting severe developmental defects.**

## INTRODUCTION

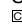
Plant cell walls are composed of structural proteins and polysaccharides such as cellulose, hemicelluloses, and pectins. L-Ara is a constituent of many different cell wall components, including pectic rhamnogalacturonan I and II, glucuronoarabinoxylans, arabinogalactan proteins, and extensins. L-Ara occurs in the furanose rather than in its thermodynamically more stable pyranose form (reviewed in Mohnen, 2008; Scheller and Ulvskov, 2010). Yet, only recently was the conversion of L-arabinopyranose (Arap) into L-arabinofuranose (Araf) during plant cell wall polysaccharide synthesis characterized. Konishi et al. (2007) demonstrated that nucleotide sugar mutases interconvert UDP-Arap and UDP-Araf in rice (*Oryza sativa*). The mutases belong to a small gene family that encodes the previously named Reversibly

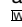
Glycosylated Proteins (RGPs), which is unrelated to the UDP-galactomutases present in some microorganisms. Until now, numerous RGPs from diverse plant species have been isolated and demonstrated to be reversibly glycosylated by nucleotide sugars such as UDP-Glc, UDP-Xyl, and UDP-Gal (Dhugga et al., 1991; Langeveld et al., 2002; De Pino et al., 2007; Konishi et al., 2007).

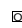
RGPs are highly conserved plant-specific cytosolic proteins that tend to associate with the Golgi membranes. Therefore, RGPs have been implicated in polysaccharide biosynthesis. Identification of the first RGP was achieved by covalent labeling of proteins with radiolabeled substrates. The identified protein was named RGP1, as it could be reversibly glycosylated, providing various UDP-sugars. The protein was localized to the trans-Golgi compartment but also found in soluble extracts, leading the authors to propose that RGP1 is made on cytosolic polysomes and associates postsynthetically with Golgi membranes as a peripheral protein. Cloning of the RGP1-encoding gene from pea (*Pisum sativum*) and generation of specific antibodies (Dhugga et al., 1991, 1997) led to the identification of putatively orthologous RGPs in various other plant species, such as *Arabidopsis thaliana* (Delgado et al., 1998), cotton (*Gossypium hirsutum*; Zhao and Liu, 2002), maize (*Zea mays*; Singh et al., 1995; Rothschild et al., 1996), potato (*Solanum tuberosum*;

<sup>1</sup> Address correspondence to hscheller@lbl.gov.

The author responsible for distribution of materials integral to the findings presented in this article in accordance with the policy described in the Instructions for Authors (www.plantcell.org) is: Henrik Vibe Scheller (hscheller@lbl.gov).

 Some figures in this article are displayed in color online but in black and white in the print edition.

 Online version contains Web-only data.

 Open Access articles can be viewed online without a subscription. www.plantcell.org/cgi/doi/10.1105/tpc.111.083931

Bocca et al., 1999), wheat (*Triticum aestivum*), rice (Langeveld et al., 2002), and tomato (*Solanum lycopersicum*; Selth et al., 2006).

Determination of a biological function of RGP has been a challenging task over the last years. Early studies implicated RGP of different species such as maize (Singh et al., 1995; Rothschild et al., 1996), potato (Bocca et al., 1999), and wheat (Langeveld et al., 2002) in starch synthesis, most likely due to their occurrence in starch-synthesizing tissues such as endosperm or potato tubers. However, this hypothesis was proven implausible, as RGP does not contain a transit peptide for targeting into plastids. Furthermore, RGP1 does not interact with ADP-Glc, a major substrate in starch synthesis in plants (Dry et al., 1992), and its biochemical properties are inconsistent with starch synthesis, as shown for the potato putative ortholog (Bocca et al., 1999). A role in cell wall biosynthesis is more likely, considering the specific association of RGP1 with the trans-Golgi compartment (Dhugga et al., 1997; Delgado et al., 1998; Bocca et al., 1999; Zhao and Liu, 2002). Zhao and Liu (2002) demonstrated that the cotton RGP gene is highly expressed during fiber development but also at the primary cell wall elongation and cell wall thickening stages, suggestive of a function in noncellulosic polysaccharide biosynthesis of the cell wall. Another clue about a possible role of RGP in plants was provided by Selth et al. (2006), whereby the interaction of RGP from tomato with the tomato leaf curl virus V1 protein implicated RGP in plant defense responses.

In *Arabidopsis*, RGP constitute a small gene family comprising five members with identities between 50 and 95% in their amino acid sequences. *Arabidopsis* RGP1 and its close homolog RGP2 have been implicated in microspore development and pollen mitosis affecting cell division and/or vacuole integrity (Drakakaki et al., 2006). Expression analysis revealed that *RGP1* and *RGP2* are highly expressed in actively growing tissues and were assumed to be required for the synthesis of large amounts of cell wall components. However, single gene disruptions did not result in obvious phenotypic alterations, suggesting functional redundancy within the *Arabidopsis* RGP family. Yet, *rgp1 rgp2* double mutants were determined to be male gametophyte lethal. More detailed analysis disclosed that mutant pollen grains have abnormally enlarged vacuoles and a poorly defined inner cell layer, leading to disintegration of the pollen structure during pollen mitosis I.

Here, we present evidence that members of the *Arabidopsis* RGP protein family constitute UDP-L-Ara mutases. Based on studies of mutant and double knockdown lines, we demonstrate that the interconversion of UDP-Arap and UDP-Araf is essential for cell wall establishment and plant development.

## RESULTS

### Spatial and Developmental Expression Patterns

The expression patterns of *Arabidopsis* RGP in various tissues such as roots, seedlings, rosette leaves, stems, inflorescences, and siliques at different developmental stages were assessed by quantitative (q) RT-PCR. *RGP1*, *RGP2*, and *RGP5* transcripts

were detected in all examined tissues, with highest amounts in flowers, seedlings, and developing siliques. In contrast, *RGP3* and *RGP4* transcripts were almost exclusively detected in siliques, with the highest levels 6 to 8 d post anthesis (Figure 1).

To obtain better spatially and developmentally resolved information on RGP expression, we stably expressed these proteins as fusion proteins carrying a C-terminal yellow fluorescent protein (YFP) tag driven by their native promoters in *Arabidopsis*. RGP1-YFP, RGP2-YFP, and RGP5-YFP proteins were detected in all major *Arabidopsis* organs (Figure 2). In immature plants, RGP1-YFP was predominantly expressed in shoot (Figure 2A) and root (Figure 2D) apical meristems. During the reproductive stage, expression was detected in pollen (Figure 2C), phloem and epidermal cells of inflorescence stems (Figure 2B), leaves (Figure 2E), and seed coat epidermal cells (Figures 2F and 2G). RGP2-YFP was predominantly expressed in the epidermis and phloem of inflorescence stems (Figure 2I), root meristems (Figure 2K), and pollen (Figure 2J). Strong YFP signals were also observed originating from leaf trichome cells of immature plants (Figure 2H), leaf epidermis (Figure 2L), and seed coat epidermal cells (Figures 2M and 2N). Similarly, RGP5-YFP appeared to be ubiquitously expressed throughout plant development (Figures 2O–2U). RGP5 expression was detected in leaves (Figure 2S), stem epidermis and phloem (Figure 2P), root vasculature as well as meristems (Figure 2R), and seed coat epidermis (Figures 2T and 2U). In contrast, RGP3 and RGP4 expression was restricted to developing seeds (Figures 2V–2Y). RGP3-YFP signals were detected in areas corresponding to the endosperm of developing seeds at the linear and bent cotyledon stage (Figures 2V and 2W). RGP4-YFP was only observed in seed coat epidermal cells of seeds at the linear to mature cotyledon stage (Figures 2X and 2Y; seed developmental stages adopted from Le et al., 2010).

### Subcellular Localization

RGP are predicted not to contain any transmembrane domain or known targeting sequence. To investigate the subcellular localizations of the *Arabidopsis* RGP, we analyzed stably and transiently expressed RGP-YFP fusions driven by their native or the constitutive cauliflower mosaic virus (CaMV) 35S promoter.

In our RGP<sub>pro</sub>:RGP-YFP approach, RGP1 and RGP2 exhibited an identical subcellular localization pattern. Both proteins localized to moving, punctate structures apparently corresponding to Golgi vesicles as well as to the cytosol (Figures 2E, 2G, 2L, and 2N). In addition, we observed RGP1-YFP and RGP2-YFP signals originating from larger particles floating within the cytosol (Figures 2E–2G and 2L–2N). RGP5-YFP appeared predominantly to be localized to the cytosol and, to a lesser extent, associated with Golgi-like particles (Figures 2S and 2U). Although RGP3-YFP and RGP4-YFP were strongly expressed in developing seeds, no conclusive information could be obtained on their subcellular localizations using this approach. The integrities and functionalities of RGP-YFP fusion proteins expressed under the control of their native promoters were confirmed by immunoblotting and enzyme activity assays using immunoprecipitated proteins (see Supplemental Figure 1 online). Further proof of functionality and correct targeting of the YFP fusion proteins was obtained by complementation analysis of *rgp1-1* and

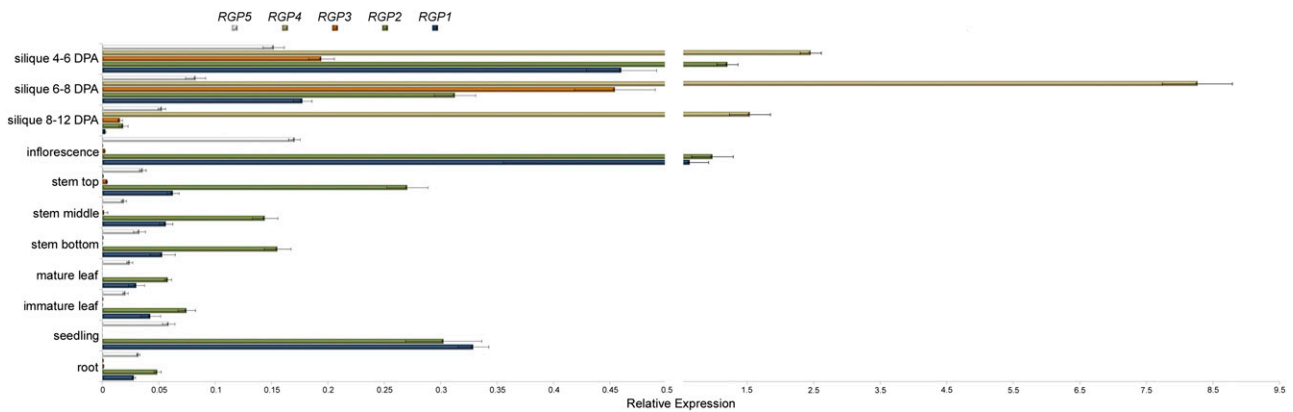


**Figure 1.** Quantitative RT-PCR Analysis of *RGP* Expression in Major *Arabidopsis* Organs and at Different Developmental Stages.

Seedlings were grown for 10 d in sterile culture. Leaves were harvested from 5-week-old plants (rosette stage; immature leaf). Other material was derived from 8-week-old flowering plants. Stems were divided into three parts, and siliques were harvested at the indicated time points. The levels of expression are calculated relative to the *UBQ10* gene, and data represent means  $\pm$  SD of three biological replicates. DPA, days post anthesis.

*rgp2-1* mutant lines. Introduction of the  $RGP1_{pro}:RGP1$ -YFP and  $RGP2_{pro}:RGP2$ -YFP constructs into the respective mutant backgrounds fully complemented their biochemical phenotypes (see Supplemental Figure 2 online).

When stably expressed under the control of the CaMV 35S promoter in *Arabidopsis*, *RGP1*-YFP, *RGP2*-YFP, *RGP3*-YFP, and *RGP4*-YFP signals could only be observed originating from larger particles floating within the cytosol, most likely corresponding to protein aggregates. By contrast, *RGP5*-YFP localization appeared to be similar to its subcellular localization pattern when expressed under the control of the native promoter (see Supplemental Figure 3 online).

When transiently expressed in tobacco (*Nicotiana benthamiana*) leaves, *RGP1*-YFP and *RGP2*-YFP fluorescence originated from Golgi-like particles as well as from the cytosol and *RGP5*-YFP appeared to be predominantly localized to the cytosol. Similarly, *RGP3*-YFP and *RGP4*-YFP fluorescence originated from Golgi-like particles and from the cytosol (see Supplemental Figure 4 online).

To obtain further information on RGP subcellular localizations, we separated plant cell extracts derived from  $RGP_{pro}:RGP$ -HA-expressing transgenic lines into cytosolic, peripheral membrane, and membrane protein fractions. As shown in Figure 3A, all five RGPs were predominantly detected in cytosolic and peripheral membrane protein fractions, and except for *RGP4*, none of the RGPs was detected in detergent-solubilized membrane fractions. As controls, cytosolic Fru-1,6-bisphosphatase (cFBPase; cytosolic protein; Strand et al., 2000), secretion-associated and Ras-related (Sar1; peripheral vesicular GTPase; Memon, 2004), and calreticulin (endoplasmic reticulum [ER] resident protein; Christensen et al., 2010) were predominantly detected in their proposed subcellular fractions. To differentiate between peripheral membrane and luminal proteins, we subjected microsomal fractions to proteinase K treatments followed by SDS-PAGE and immunoblotting. Whereas all five RGPs were detected in untreated microsomal fractions, proteinase K treatment completely degraded the corresponding proteins. As a control, calreticulins

were protected from degradation, indicative for intactness of ER cisternae and Golgi vesicles under our experimental conditions (Figure 3B).

### Enzymatic Activities Identified *Arabidopsis* RGPs as UDP-Ara Mutases

The five *Arabidopsis* RGPs were heterologously expressed as hexahistidine tag fusion proteins in *Escherichia coli* and affinity purified for subsequent enzymatic assays. Immunoblot analysis of the purified proteins revealed two predominant bands for each protein detected by the anti-hexahistidine antibody within the range of  $\sim$ 45 to 50 kD, which is in agreement with their predicted molecular masses (*RGP1*, 40.6 kD; *RGP2*, 40.9 kD; *RGP3*, 41.3 kD; *RGP4*, 41.9 kD; *RGP5*, 38.6 kD; plus C-terminal peptide containing the V5 epitope and the polyhistidine tag of  $\sim$ 4 kD; Figure 4A). Recombinant proteins were tested for UDP-Ara mutase activity as described by Konishi et al. (2007). As substrates, we provided either UDP-Arap or UDP-Araf. The corresponding reaction products were separated by HPLC and subsequently identified by electrospray ionization-mass spectrometry (ESI-MS). Mutase activity was observed for recombinant *RGP1*, *RGP2*, and *RGP3*. In contrast, HPLC analyses of enzymatic reactions containing recombinant *RGP4* or *RGP5* did not reveal any additional peaks compared with control reactions (Figures 4C and 4D). When UDP-Araf was used as a substrate, a rapid conversion into UDP-Arap was detected for recombinant *RGP1*, *RGP2*, and *RGP3*, with activities  $RGP1 > RGP2 \geq RGP3$  (Figure 4D). When UDP-Arap was used as a substrate, only small amounts ( $\sim$ 5%) were converted into UDP-Araf by the active enzymes (Figure 4C), consistent with a thermodynamic equilibrium of 9:1 as observed in rice (Konishi et al., 2007, 2010). LC-ESI-MS analysis of the UDP-Arap and UDP-Araf peaks identified these compounds with a molecular mass  $[M-H]^-$  of 535.35 and 535.36, respectively, which is consistent with the calculated theoretical mass  $[M-H]^-$  of 535.28 (Figures 4E and 4F). When other UDP-sugars (UDP-Gal, UDP-Xyl, UDP-Glc, GDP-Man,

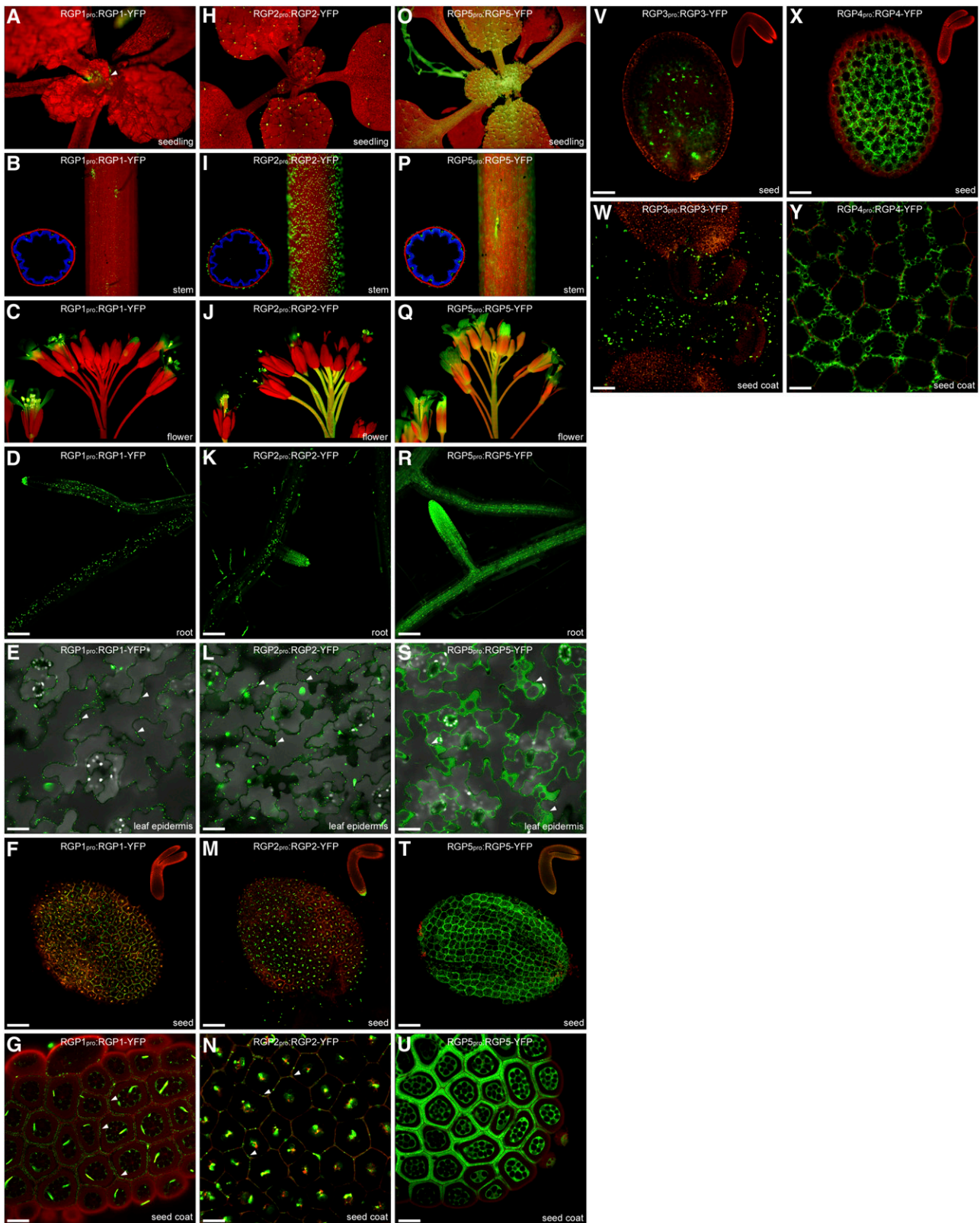


Figure 2. RGP<sub>pro</sub>:RGP-YFP Expression Pattern in Transgenic *Arabidopsis* Plants.

and GDP-Fuc) were provided as substrate, no additional peaks or reduction of the corresponding substrate was observed when reacted with any of the recombinant RGP proteins or mixtures thereof. The specificity for UDP-Ara is in contrast to the flavin adenine dinucleotide-containing UDP-Gal mutases known from several microorganisms, which have activity with both UDP-D-Gal and UDP-L-Ara (Zhang and Liu, 2001).

### Protein Complex Formation

RGPs from various plant species have been demonstrated to form homoprotein or heteroprotein complexes (Langeveld et al., 2002; Drakakaki et al., 2006; De Pino et al., 2007). To investigate the *Arabidopsis* RGPs regarding protein complex formation, composition, and enzymatic activities, we stably expressed the corresponding proteins in *Arabidopsis* as translational hemagglutinin (HA) tag fusions under the control of their native promoters. The RGP-HA proteins were subsequently immunoprecipitated from total protein extracts derived from seedlings (RGP1-HA, RGP2-HA, and RGP5-HA; similar results were obtained using leaf or flower protein extracts) or protein extracts derived from developing siliques (RGP3-HA and RGP4-HA). SDS-PAGE separation followed by Sypro Ruby protein gel staining revealed multiple bands in each of the RGP-HA immunoprecipitates with at least three components, which is indicative of an association in a protein complex (Figure 5A). Immunoblots detected the corresponding HA-tagged polypeptide as a single band in each of the five RGP-HA extracts (Figure 5B). LC-ESI-MS/MS was used to identify the corresponding complex components in in-solution tryptic digested extracts. Unambiguously identified proteins (sequence coverage > 10% and at least one unique peptide match for a certain RGP protein) are listed in Table 1 and peptide sequences in Supplemental Table 1 online. When RGP1-HA was used as bait, RGP2 and RGP5 were coprecipitated. Reciprocal interactions were observed for RGP2-HA (coimmunoprecipitated with RGP1 and RGP5) and RGP5-HA (coprecipitated with RGP1 and RGP2) pull-down experiments. In protein samples derived from developing siliques expressing RGP3-HA, RGP1 coprecipitated with the tagged RGP3 protein. RGP1 and RGP2 were coprecipitated when the RGP4-HA protein was used as bait.

Immunoprecipitated protein complexes were tested for UDP-Ara mutase activity with UDP-Arap (see Supplemental Figure 5 online) and UDP-Araf (Figure 5C) as substrates. HPLC analysis of the corresponding reaction products revealed mutase activity in all five immunoprecipitated extracts (Figure 5C), which supports our proteomic data demonstrating the existence of at least one active mutase in each protein complex.

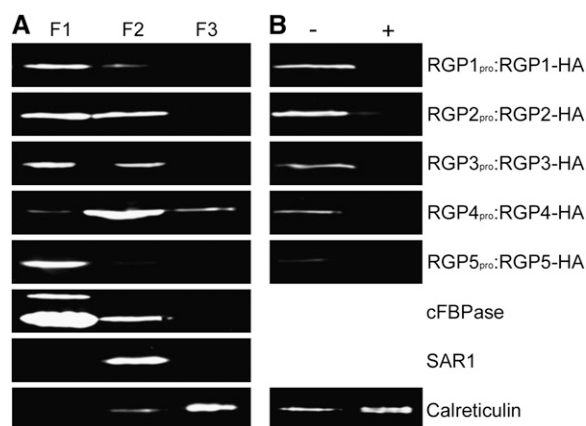


**Figure 3.** Subcellular Localizations of the *Arabidopsis* RGP Proteins.

**(A)** Subcellular protein fractionation of RGP<sub>pro</sub>:RGP-HA-expressing transgenic plants. F1, cytosolic fraction; F2, alkali-released peripheral membrane proteins; F3, detergent-solubilized membrane fraction.

**(B)** Proteinase K protection assay. Microsomal fractions were treated with (+) or incubated without (-) proteinase K before detergent solubilization and analyzed by SDS-PAGE and immunoblotting.

### *Arabidopsis* Lines with Reduced RGP Expression Are Deficient in Cell Wall Ara

*RGP1* and *RGP2* were previously proposed to act redundantly in pollen development. Double knockouts were determined to be male gametophyte lethal, with an arrest in pollen mitosis, whereas single mutants did not exhibit phenotypic alterations compared with wild-type plants (Drakakaki et al., 2006). However, single mutant lines have not been analyzed with regard to their cell wall monosaccharide composition. To further characterize RGP function and the impact of UDP-Arap/UDP-Araf interconversion on plant development, we analyzed single *RGP1* and *RGP2* mutants and created a hairpin (hp) construct (named hpRGP1/2) specifically targeting *RGP1* and *RGP2* expression. Two independent *RGP1* mutant lines, *rgp1-1* and *rgp1-2*, carrying a T-DNA insertion either in the first or the third intron, respectively, were identified in the GABI-KAT collection (Rosso et al., 2003), and two independent *RGP2* mutant alleles, *rgp2-1* and *rgp2-2*, carrying a T-DNA insertion in the third exon or the first intron, respectively, were identified in the SIGnAL collection (Alonso et al., 2003). Plants carrying homozygous insertions were selected by PCR. The effect of the T-DNA insertion on mRNA expression levels was examined using qRT-PCR. No transcripts were detected in homozygous *rgp1-1* and *rgp2-2* individuals, and >90% reductions in transcript amounts were determined for

**Figure 2.** (continued).

RGPs were stably expressed in *Arabidopsis* as C-terminal translational YFP fusion proteins under the control of their native promoters. Two-week-old plants are shown in **(A)**, **(H)**, and **(O)**. Inflorescence stems and cross sections with blue and red color indicating autofluorescence upon UV light excitation are shown in **(B)**, **(I)**, and **(P)**. Inflorescences **(C)**, **(J)**, and **(Q)**, roots **(D)**, **(K)**, and **(R)**, and single-plane confocal micrographs of leaf epidermis of rosette-stage plants **(E)**, **(L)**, and **(S)** are also shown. Developing seed and embryo **(F)**, **(M)**, **(T)**, **(V)**, **(W)**, and **(X)** and seed coats of developing seeds **(G)**, **(N)**, **(U)**, and **(Y)** are shown. Arrows indicate Golgi vesicles. Bars = 100  $\mu$ m **(D)**, **(K)**, **(R)**, **(F)**, **(M)**, **(T)**, **(V)**, **(W)**, and **(X)** and 25  $\mu$ m **(E)**, **(L)**, **(S)**, **(G)**, **(N)**, **(U)**, and **(Y)**.

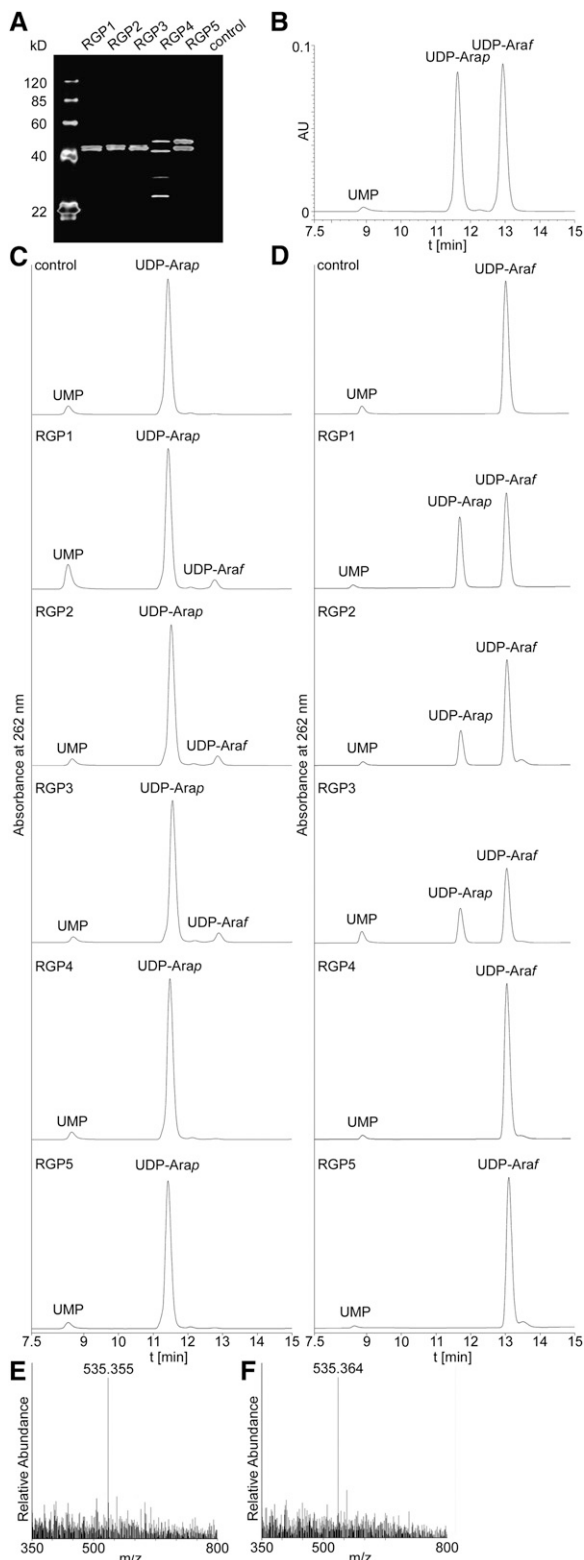


**Figure 4.** UDP-Ara Mutase Activities of Recombinant *Arabidopsis* RGP Proteins.

(A) Immunoblot analysis of purified recombinant RGP proteins expressed in *E. coli*.

plants carrying the *rgp1-2* and *rgp2-1* alleles (Figure 6A). Even though single knockout lines did not show any growth phenotypic alterations compared with accession Columbia-0 (Col-0) wild-type plants, cell wall monosaccharide analysis revealed a significant reduction in total cell wall Ara content in *RGP1* mutants (*rgp1-1*,  $16.0\% \pm 0.3\%$ ,  $P \leq 0.001$ ; *rgp1-2*,  $12\% \pm 5\%$ ,  $P \leq 0.01$ ) and *RGP2* mutants (*rgp2-1*,  $29\% \pm 8\%$ ,  $P \leq 0.001$ ; *rgp2-2*,  $30\% \pm 2\%$ ,  $P \leq 10^{-5}$ ; Figure 6B). Other cell wall sugars were not significantly altered when compared with the Col-0 wild type (see Supplemental Table 2 online). Consistently, determination of UDP-Ara mutase activities in cytosolic and microsomal protein extracts using UDP-Araf as substrate revealed about a 50% reduction in *rgp1* and *rgp2* mutants compared with the Col-0 wild type (Table 2). This was further corroborated by quantifying UDP-Arap, UDP-Xyl, and UDP-Glc in *rgp1* and *rgp2* plant seedlings. Indeed, in the mutant plants, UDP-Arap was increased by  $\sim 42$  and 67% in the *rgp1* and *rgp2* mutants, respectively. Moreover, the direct precursor of UDP-Arap, UDP-Xyl, was also increased in these mutants. Traces of UDP-Araf could be found both in the mutant lines as well as in the wild type and hinted at a reduction in the mutant lines, but amounts were below the limit of quantification (Table 3).

To examine the consequences of a simultaneous downregulation of *RGP1* and *RGP2* expression on cell wall monosaccharide composition and developmental phenotype habits, we generated plant lines expressing a hairpin construct specifically targeting *RGP1* and *RGP2* expression. qRT-PCR analysis of nine randomly selected independent transgenic individuals revealed three classes of lines with varying degrees of *RGP1* and *RGP2* expression (Figure 6A). The first class contained lines with slightly reduced expression or expression levels similar to control plants transformed with an empty vector (hpRGP1/2-6), the second class contained plants with an intermediate (37–90%) reduction in expression (hpRGP1/2-2, -5, -4, -8, and -3), and the third class was represented by lines with a strong (90–97%) reduction in *RGP1* and *RGP2* expression (hpRGP1/2-1, -7, and -9). As shown in Figure 6A, expression of *RGP5* was not affected in hpRGP1/2 lines. Subsequent monosaccharide analysis of cell wall polysaccharide extracts derived from hpRGP1/2 lines revealed a strong correlation between the level of *RGP1/RGP2* expression and total cell wall Ara content (*RGP1*,  $r = 0.88$ ; *RGP2*,  $r = 0.94$ ; average,  $r = 0.92$ ; Figure 6C). Up to an  $\sim 80\%$  reduction in cell wall polysaccharide Ara content was measured for the hpAtRGP1/2-1, -7, and -9 lines, which exhibited the strongest reduction in *RGP1* and *RGP2* expression (Figures 6A and 6B; see Supplemental Table 3 online). Moreover, the reduction in *RGP1* and *RGP2* expression and correspondingly reduced cell wall Ara content was accompanied by severe developmental defects compared with control lines (Figure 6D). Plants with a 60 to 90%

(B) HPLC separation of authentic UDP-Arap and UDP-Araf standards.

(C) HPLC chromatograms of products formed after reaction of UDP-Arap with the corresponding recombinant *Arabidopsis* enzyme.

(D) HPLC chromatograms of products formed after reaction of UDP-Araf with the corresponding recombinant *Arabidopsis* enzyme.

(E) and (F) ESI-MS spectra of UDP-Araf at time 0 (E) and UDP-Araf at 10 min (F), when UDP-Araf was reacted with recombinant RGP1.

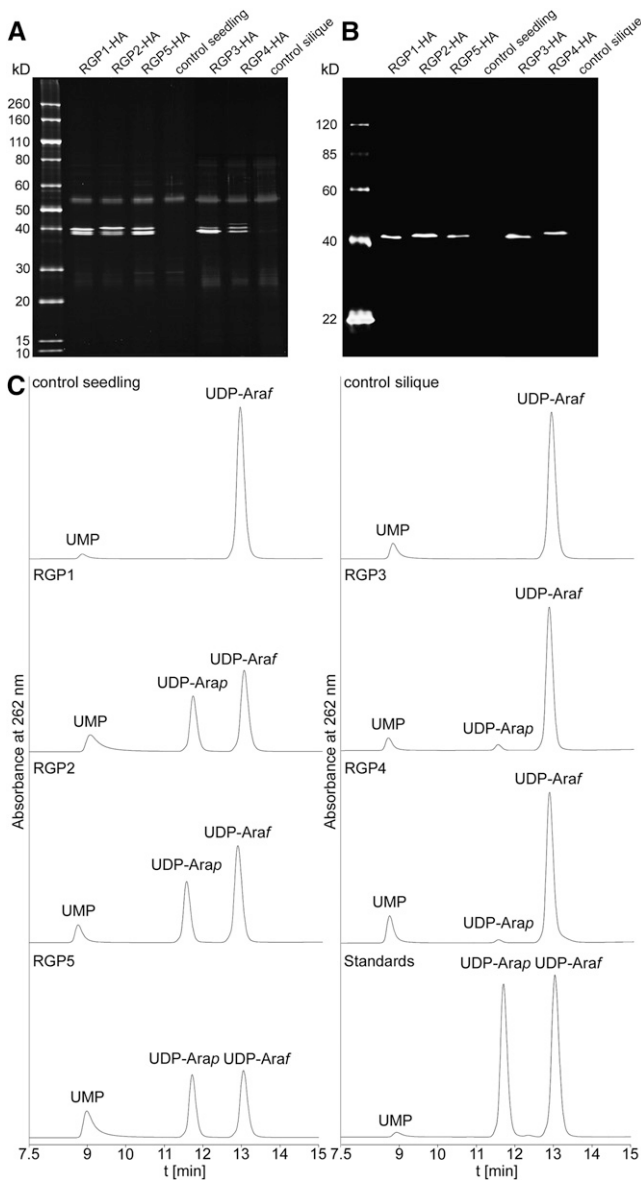


**Figure 5.** The *Arabidopsis* RGPs Are Associated in Heteroprotein Complexes.

HA-tagged RGP proteins were stably expressed in *Arabidopsis* under the control of their native promoters and subsequently immunoprecipitated. **(A)** SDS-PAGE separation of immunoprecipitated protein complexes visualized with Sypro Ruby protein gel stain.

**(B)** Corresponding immunoblot probed with an anti-HA antibody detecting single bands in each RGP-HA extract.

**(C)** Mutase activities of RGP complexes determined using UDP-Araf as substrate.

(*RGP1*) and 37 to 83% (*RGP2*) reduction in expression, resulting in a 9 to 42% reduction in Ara content, were phenotypically indistinguishable from control plants. In contrast, hp*RGP1/2-1*, -7, and -9 lines with reductions of  $\geq 94$  and  $\geq 87\%$  in *RGP1* and *RGP2* expression, respectively, and a subsequent reduction in total cell wall Ara of  $\geq 69\%$  were severely developmentally

retarded, resulting in dwarf phenotypes (Figure 6D). Notably, the majority of all hp*RGP1/2* transgenic lines showed arrested development and died immediately after selection. Determination of UDP-Ara mutase activities in cytosolic and microsomal protein extracts using UDP-Araf as substrate revealed  $>95\%$  reduction in hp*RGP1/2* lines compared with control lines transformed with an empty vector (Table 2).

Analysis of sugar composition in cell wall preparations from wild-type (empty vector control [EVC]) and hp*RGP1/2* lines suggested a slightly altered composition besides the 83% reduction in Ara (Table 4, total; two-way analysis of variance [ANOVA],  $P < 0.003$ ). A closer inspection indicated that Gal and Rha were disproportionately increased in the hp*RGP1/2* lines. To further investigate the impact of reduced UDP-Arap/UDP-Araf interconversion on different cell wall polymers, we extracted the cell wall preparations sequentially with cyclohexanediamine-tetraacetic acid (CDTA) and  $\text{Na}_2\text{CO}_3$ . The 80 to 90% decrease in L-Ara was similar in all fractions (Table 4). Neither the CDTA fraction nor the  $\text{Na}_2\text{CO}_3$  fraction from the hp*RGP1/2* lines showed any significant differences in sugar composition besides the decrease in Ara. In contrast, the increase in Gal and Rha observed in the total cell wall preparations was also evident in the residue after extraction with CDTA and  $\text{Na}_2\text{CO}_3$ . Furthermore, while GalA content did not differ in total amount, it showed a significantly different extractability between the control and hp*RGP1/2* lines (two-way ANOVA,  $P < 0.0007$ ). These observations indicate that the plants respond to the decrease in Ara (including pectic arabinan) by increasing rhamnogalacturonan I (RG I) polymers. However, RG I in the hp*RGP1/2* walls is less easily extracted.

Since L-Ara in arabinan side chains is a major constituent of pectin and the mucilage secretory cells of the *Arabidopsis* seed coat constitute a prominent model system for cell wall establishment, in particular for pectin synthesis and modification (reviewed in Arsovski et al., 2010), we analyzed hp*RGP1/2*-derived seeds for mucilage extrusion. The seed mucilage can be visualized by staining with ruthenium red (Hanke and Northcote, 1975). Staining of water-imbibed hp*RGP1/2* mutant seeds derived from lines -7 and -9, which had the greatest reduction in Ara contents, revealed an immediate solubilization of the outer mucilage and only faint staining of the inner mucilage. In contrast, wild-type (EVC) and hp*RGP1/2-1* seeds showed intense spherical staining of the inner and outer mucilage, which was still attached to the seed (Figure 6E).

Since we found *RGP5* to be a third component of the *RGP1/RGP2* protein complex, we created a hairpin construct specifically targeting *RGP5* expression (named hp*RGP5*). However, repression of *RGP5* expression to as low as 15% of the wild-type level in nine randomly selected transgenic lines (see Supplemental Figure 6 online) did not result in any morphological alterations or significant differences in the cell wall monosaccharide composition (Figure 6B; see Supplemental Table 3 online).

## DISCUSSION

We demonstrated that *Arabidopsis RGP1*, *RGP2*, and *RGP5* are ubiquitously expressed throughout plant development, whereas *RGP3* and *RGP4* expression is restricted to seed

**Table 1.** Identified Protein Complex Components in RGP Immunoprecipitates

Bait	Prey	Score	MW (D)	PM	Cov (%)
RGP1-HA	RGP1	292	40,602	12	34.2
	RGP2	130	40,864	9	23.6
	RGP5	38	38,560	5	14.4
RGP2-HA	RGP2	189	40,864	10	25.6
	RGP1	158	40,602	8	25.8
	RGP5	152	38,560	4	12.4
RGP5-HA	RGP5	454	38,560	14	37.4
	RGP1	194	40,602	12	37.8
	RGP2	157	40,864	12	31.9
RGP3-HA	RGP3	74	41,254	7	17.4
	RGP1	37	40,602	4	12
	RGP4	178	41,839	14	35.7
RGP4-HA	RGP1	57	40,602	5	12
	RGP2	44	40,864	5	11.7

RGPs were stably expressed in *Arabidopsis* as translational HA tag fusion proteins driven by their native promoters. Immunoprecipitated protein complexes were tryptic digested in solution and subsequently analyzed by LC-ESI-MS/MS. MW, molecular mass; PM, number of peptides matched; Cov, protein sequence coverage.

development. From enzymatic assays of recombinant RGP proteins expressed in *E. coli*, three *Arabidopsis* enzymes were identified as UDP-Ara mutases. We have shown that single *RGP1* and *RGP2* knockout mutants exhibit a significant reduction in cell wall Ara content. The interconversion of UDP-Arap and UDP-Araf appeared to be indispensable for plant development, as *RGP1* and *RGP2* double knockdowns showed severe developmental retardation and dwarf phenotypes. Moreover, we identified all five *Arabidopsis* RGPs as being associated in heteroprotein complexes that always contain at least one active UDP-Ara mutase component.

### The *Arabidopsis* RGPs Have Distinct but Overlapping Expression Patterns

We presented the spatial and developmental expression patterns of all five *Arabidopsis* RGPs as determined by qRT-PCR and RGP<sub>pro</sub>:RGP-YFP fusions stably expressed in *Arabidopsis*. Both approaches consistently demonstrated the ubiquitous expression of RGP1, RGP2, and RGP5 throughout plant development, indicative of a general function in plant cell wall metabolism. In contrast to RGP5, which displayed near constant expression levels, the expression levels of RGP1 and RGP2 varied to some extent in different organs. Expression was strongest in meristematic and developing tissues, where cell division and expansion requires large amounts of substrates for glycan synthesis. Similar expression patterns have been previously reported for *Arabidopsis* RGP1 and RGP2 (Drakakaki et al., 2006), pea RGP (Dhugga et al., 1991), and maize RGP (Sagi et al., 2005).

Interestingly, in all analyzed *Arabidopsis* organs, the cytoplasmic RGP1-YFP and RGP2-YFP signals were present partially as larger fluorescent particles. Recently, similar particles have been detected in *Arabidopsis* by the LM6 antibody, which specifically

recognizes  $\alpha$ -(1→5)-L-arabinans (Willats et al., 2001; Gomez et al., 2009). The authors speculated that soluble heteroglycans, which have been reported to be rich in Ara (Fettke et al., 2005), were the epitope for this large cytoplasmic labeling. Therefore, it is tempting to speculate that RGPs are associated with and/or involved in the synthesis of soluble heteroglycans.

qRT-PCR and RGP<sub>pro</sub>:RGP-YFP fusions revealed restricted but strong expression of RGP3 and RGP4 during seed development. RGP3 appeared to be deposited to the endosperm, as evident from our RGP3<sub>pro</sub>:RGP3-YFP approach. The endosperm is thought to nourish and protect the growing embryo (De Smet et al., 2010), and large amounts of Ara (up to 40% of the total monosaccharide composition of noncellulosic polysaccharides) are present in the cell walls of *Arabidopsis* embryos (Gomez et al., 2009). Surprisingly, none of the UDP-Arap mutases appeared to be strongly expressed within the embryo (except for RGP2, which is present in the root meristem). Thus, RGP3 might be involved in Ara supply for the growing cell wall of the developing embryo delivered via the endosperm. RGP4-YFP expression was restricted to seed coat epidermal cells throughout seed development, which is indicative of a possible biological function for RGP4 in seed coat polysaccharide synthesis. Although the ABRC lists mutants in *RGP3* and *RGP4*, so far we were not able to confirm any T-DNA insertion in these lines. RNA interference approaches might be useful for assigning a certain function to *RGP3* and *RGP4* in seed development and maturation.

Our qRT-PCR data as well as information on RGP expression obtained from our RGP<sub>pro</sub>:RGP-YFP approach for *RGP3*, *RGP4*, and *RGP5* are largely consistent with publicly available microarray data (<http://bar.utoronto.ca/efp/cgi-bin/efpWeb.cgi>; Winter et al., 2007). *RGP1* and *RGP2* expression are not reliably distinguishable on the Affymetrix ATH1 array, with both transcripts cross-hybridizing with the present probe sets.

### The *Arabidopsis* RGPs Are Cytosolic Proteins

In previous studies, RGPs were localized to several subcellular compartments, including the cytosol (Dhugga et al., 1991; Drakakaki et al., 2006), Golgi (Drakakaki et al., 2006), and plasmodesmata (Sagi et al., 2005). Our RGP<sub>pro</sub>:RGP-YFP approach demonstrated that RGP1, RGP2, and RGP5 are present in the cytosol and associated with Golgi-like particles where cell wall polysaccharides are assembled. Complementation studies by introducing the RGP1<sub>pro</sub>:RGP1-YFP or RGP2<sub>pro</sub>:RGP2-YFP construct into the respective *rgp1-1* or *rgp2-1* single mutant line proved the functionalities and proper targeting of the respective YFP fusion proteins. Although *Arabidopsis* RGPs ectopically expressed in tobacco plants have been localized to plasmodesmata (Sagi et al., 2005), we did not observe any fluorescence originating from plasmodesmata, consistent with previous studies in *Arabidopsis* (Dhugga et al., 1997; Delgado et al., 1998; Drakakaki et al., 2006).

Subcellular protein fractionation experiments and proteinase K protection assays confirmed a cytosolic localization and revealed a peripheral membrane association of all five *Arabidopsis* RGPs. Under our experimental conditions, peripheral proteins were stripped off the membranes by carbonate



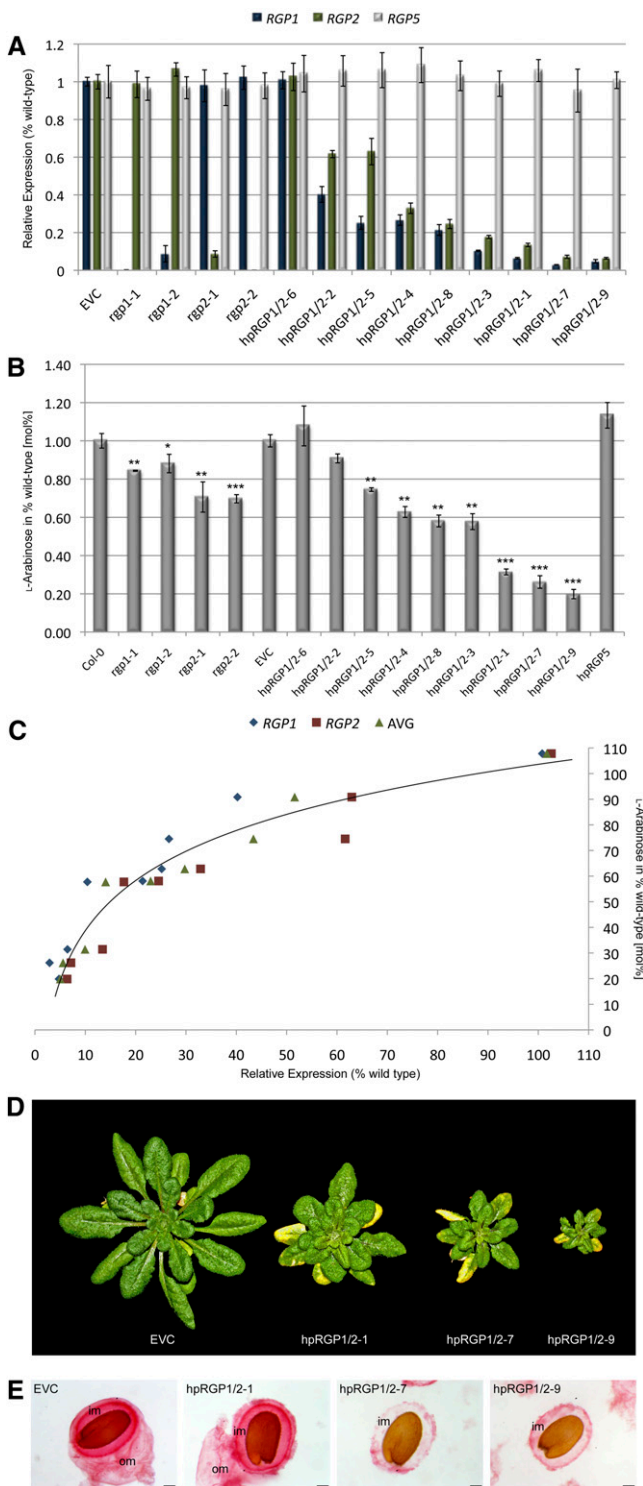


**Figure 6.** UDP-Araf Supply in *Arabidopsis* Depends on RGP1 and RGP2.

**(A)** qRT-PCR analysis of *RGP* expression in control plants transformed with an empty vector (EVC), *rgp1-1*, *rgp1-2*, *rgp2-1*, and *rgp2-2* single mutants, and nine transgenic individuals expressing a hairpin construct specifically targeting *RGP1* and *RGP2* (hpRGP1/2) expression. Express-

ion values were determined for *RGP1*, *RGP2*, and *RGP5* and are expressed relative to the wild-type (EVC), which was set to 1. Data represent means  $\pm$  SD of three biological replicates. **(B)** Ara contents of cell wall polysaccharides expressed as a percentage of the wild-type value (mol %). Col-0 represents plants transformed with an empty vector. For hpRGP5, the values represent averages  $\pm$  SD of nine independent lines. \*  $P \leq 0.01$ , \*\*  $P \leq 0.001$ , \*\*\*  $P \leq 0.0001$ . **(C)** Correlation of *RGP1* and *RGP2* expression and Ara contents in hpRGP1/2 lines. **(D)** Representative morphological phenotypes of hpRGP1/2 rosette-stage plants compared with control plants transformed with an empty vector (EVC). **(E)** Ruthenium red stains of wild-type (EVC) and hpRGP1/2 seed mucilage. The extruded mucilage appears as a red halo. im, inner mucilage; om, outer mucilage. Bars = 100  $\mu$ m.

extraction. Treatment of isolated membranes with alkaline solutions generally removes all but integral membrane or glycosylphosphatidylinositol-anchored proteins (Fujiki et al., 1982). Except for RGP4, all RGPs were quantitatively recovered in the supernatant after alkaline extraction and ultracentrifugation. Since alkaline treatment may release cisternal contents and to assess a possible localization within the Golgi lumen, we performed proteinase K protection assays. All five RGPs were effectively degraded when membrane-enriched fractions were treated with proteinase K, which is indicative of a peripheral membrane association of RGPs. To ensure the intactness of the isolated membranes, we performed control reactions using an anti-calreticulin antibody. Calreticulins are highly conserved proteins that contain an ER retention signal and are retained within the ER lumen by an interaction with the KDEL receptor (Munro and Pelham, 1987), but they have also been found within the Golgi lumen (Jia et al., 2009). Since we detected calreticulins in proteinase-treated and untreated membrane fractions, we concluded that cisternae and vesicles were intact and not excessively broken under our experimental conditions.

### The *Arabidopsis* RGP Family Consists of Three UDP-Ara Mutases and Two Nonmutases

The predominant presence of all five RGPs in cytosolic fractions, their degradation in proteinase protection assays, and the absence of any predicted transmembrane domain and targeting sequence in their amino acid sequences provide evidence for a cytosol-oriented association of RGPs with Golgi vesicular membranes. Furthermore, the absence in solubilized membrane fractions provides further evidence that RGPs can be associated with but do not penetrate the hydrophobic membrane. This conclusion regarding subcellular localization is consistent with previous observations, where isolation of Golgi from mung bean (*Vigna radiata*) led to the loss of UDP-Ara mutase activity (Konishi et al., 2006).

Recently, the rice RGPs rUAM1 and rUAM3 were purified from plant material as well as heterologously expressed in *E. coli* and insect cells, respectively. Both the native and the recombinant proteins have been demonstrated to interconvert UDP-Arap and UDP-Araf (Konishi et al., 2007, 2010). To examine the enzymatic activities of the corresponding putatively orthologous *Arabidopsis* RGPs, we expressed all five proteins as hexahistidine tag fusion proteins in

sion values were determined for *RGP1*, *RGP2*, and *RGP5* and are expressed relative to the wild-type (EVC), which was set to 1. Data represent means  $\pm$  SD of three biological replicates.

**(B)** Ara contents of cell wall polysaccharides expressed as a percentage of the wild-type value (mol %). Col-0 represents plants transformed with an empty vector. For hpRGP5, the values represent averages  $\pm$  SD of nine independent lines. \*  $P \leq 0.01$ , \*\*  $P \leq 0.001$ , \*\*\*  $P \leq 0.0001$ . **(C)** Correlation of *RGP1* and *RGP2* expression and Ara contents in hpRGP1/2 lines. **(D)** Representative morphological phenotypes of hpRGP1/2 rosette-stage plants compared with control plants transformed with an empty vector (EVC). **(E)** Ruthenium red stains of wild-type (EVC) and hpRGP1/2 seed mucilage. The extruded mucilage appears as a red halo. im, inner mucilage; om, outer mucilage. Bars = 100  $\mu$ m.

**Table 2.** Mutase Activities in *rgp1*, *rgp2*, and hpRGP1/2 Lines

Line	Relative Mutase Activities	
	Cytosolic	Microsomal
Col-0	100 (6.1)	100 (19)
<i>rgp1-1</i>	50.5 <sup>a</sup> (1.7)	50 <sup>b</sup> (12)
<i>rgp1-2</i>	50.1 <sup>a</sup> (1.3)	50 <sup>b</sup> (15)
<i>rgp2-1</i>	55.0 <sup>a</sup> (5.1)	39 <sup>b</sup> (12)
<i>rgp2-2</i>	59.8 <sup>a</sup> (10.8)	51 <sup>b</sup> (16)
EVC	100 (10.5)	100 (15.0)
hpRGP1/2-1	2.1 <sup>a</sup> (1.4)	1.4 <sup>a</sup> (0.4)
hpRGP1/2-7	1.8 <sup>a</sup> (0.8)	1.4 <sup>a</sup> (0.4)
hpRGP1/2-9	1.4 <sup>a</sup> (0.3)	0.9 <sup>a</sup> (0.2)

Mutase activities were measured in cytosolic and microsomal protein extracts with UDP-Araf as substrate and expressed in percentage relative to the corresponding wild-type control (Col-0; EVC). The values represent averages of three biological replicates ( $\pm$ SD). The activities of transformants and Col-0 were compared by *t* test.

<sup>a</sup>Significance at the 0.01% level.

<sup>b</sup>Significance at the 1% level.

*E. coli*. Subsequent activity assays identified RGP1, RGP2, and RGP3 as UDP-Ara mutases, able to interconvert UDP-Arap and UDP-Araf. In contrast, recombinant RGP4 and RGP5 did not show UDP-Ara mutase activities. A similar subdivision into UDP-Ara mutases and closely related homologous nonmutases has been described for the rice RGP protein family that consists of two UDP-Ara mutases (rUAM1 and rUAM3) and rUAM2, a close relative without detectible mutase activity (Konishi et al., 2007, 2010).

To further assess the relation of the *Arabidopsis* RGPs and their corresponding enzyme activities to other known and putative plant RGPs, we performed a phylogenetic analysis. Knowledge of phylogenetic relationships may help to unravel the main functions of genes based on annotation transfer from orthologous sequences. BLAST searches using *Arabidopsis* RGP full-length amino acid sequences revealed 60 nonredundant RGP-encoding genes distributed in monocots, dicots, *Physcomitrella*, *Selaginella*, and *Chlamydomonas*. A multiple sequence alignment was performed to elucidate the phylogenetic relationships within the plant RGP family (see Supplemental Data Set 1 online). The obtained neighbor-joining tree identified two major clusters of orthologous groups. Group 1 contains the previously described class 1 RGPs and includes Os\_RGP1 (rUAM1) and Os\_RGP3 (rUAM3) and *Arabidopsis* RGP1, RGP2, and RGP3. The second group represents the class 2 RGPs, including Os\_RGP2 (rUAM2) and *Arabidopsis* RGP4 and RGP5 (Figure 7; see Supplemental Data Set 1 online). Based on our UDP-Ara mutase activity data of the *Arabidopsis* RGPs and published data about the corresponding rice RGP protein family (Konishi et al., 2007), we propose that class 1 RGPs most likely represent UDP-Ara mutases, whereas class 2 comprises closely related RGPs without mutase activity.

### The *Arabidopsis* RGPs Are Associated in Heteroprotein Complexes

Several RGPs from wheat, rice, potato, and *Arabidopsis* have been proposed to be associated in homoprotein and hetero-

protein complexes (Langeveld et al., 2002; Drakakaki et al., 2006; De Pino et al., 2007). To investigate the *Arabidopsis* RGPs regarding protein complex formation, complex composition, and enzymatic activities, we stably expressed all five RGPs in *Arabidopsis* as translational HA tag fusion proteins under the control of their native promoters. Immunoprecipitations from plant seedling, leaf, or flower protein extracts with RGP1-HA, RGP2-HA, or RGP5-HA as bait and subsequent LC-MS/MS analysis unambiguously identified all three RGP proteins to be coimmunoprecipitated with each bait, suggesting that RGP1, RGP2, and RGP5 are able to form a heteroprotein complex.

Mutase activity assays using UDP-Araf as substrate and the corresponding plant extracted RGP protein complexes confirmed the existence of at least one UDP-Ara mutase in each extraction, providing further evidence for a possible interaction *in vivo*. In addition, and as a prerequisite for a possible interaction *in vivo*, RGP1, RGP2, and RGP5 exhibited largely overlapping expression patterns, as determined by RGP<sub>pro</sub>:RGP-YFP fusions. Moreover, all three RGPs are localized to the same subcellular compartments, specifically, to Golgi-like vesicles as well as to the cytosol.

The biological relevance of the existence of RGPs in protein complexes remains a mystery. Konishi et al. (2010) provided some evidence for a minor synergistic effect on mutase activity when combining different recombinant rice RGP proteins. An increase of 1.3- or 2.1-fold in mutase activities has been observed when the nonmutase rUAM2 was combined with rUAM1 or rUAM3, respectively. In our experiments, we did not observe increased activities when combining different recombinant RGPs or higher enzymatic activities of plant extracted RGP protein complexes when using UDP-Arap or UDP-Araf as substrate.

Since RGP is both observed as soluble proteins and associated with Golgi vesicles, it seems reasonable to assume that the proteins can interact with proteins in the Golgi membrane. That could also allow channeling of the UDP-Araf substrate to the arabinosyltransferases required for polysaccharide and glycoprotein synthesis. However, we did not observe any significant presence of other Golgi proteins associated with the RGP complexes. This result contrasts with the observations of Zeng et al. (2010), who found RGP associated with glycosyltransferases in wheat that are likely to be involved in arabinoxylan biosynthesis, and of Porchia et al. (2002), who showed that isolated wheat Golgi has the ability to incorporate arabinofuranose into xylan

**Table 3.** UDP-Sugar Contents in the Col-0 Wild-Type and *rgp1* and *rgp2* Mutant Lines

Line	UDP-Sugar Content (pmol/mg)			
	UDP-L-Arap	UDP-L-Araf	UDP-D-Xyl	UDP-D-Glc
Col-0	4.4 (0.5)	0.16 (0.03)	1.4 (0.3)	46 (8)
<i>rgp1-1</i>	6.3 <sup>a</sup> (1.2)	0.12 (0.06)	2.4 <sup>a</sup> (0.2)	46 (3)
<i>rgp2-1</i>	7.3 <sup>a</sup> (1.0)	0.10 (0.08)	2.7 <sup>a</sup> (0.5)	55 (3)

The values represent averages of three or more biological replicates ( $\pm$ SD).

<sup>a</sup>Significance at the 1% level.

**Table 4.** Monosaccharide Composition of Plant Cell Wall Polysaccharide Fractions Derived from the Wild-Type (EVC) and hpRGP1/2 Lines

Sugar	Total Monosaccharides/Fractionation															
	Total				CDTA				Na <sub>2</sub> CO <sub>3</sub>				Residue			
	EVC		hpRGP1/2		EVC		hpRGP1/2		EVC		hpRGP1/2		EVC		hpRGP1/2	
	μg/mg	mol %	μg/mg	mol %	μg/mg	mol %	μg/mg	mol %	μg/mg	mol %	μg/mg	mol %	μg/mg	mol %	μg/mg	mol %
Fuc	2.9 (0.2)	0.9 (0.0)	3.1 (0.1)	1.1 (0.1)	0.3 (0.0)	0.7 (0.0)	0.3 (0.1)	0.8 <sup>a</sup> (0.0)	0.2 (0.0)	0.8 (0.1)	0.2 (0.0)	0.8 (0.0)	2.4 (0.5)	3.5 (0.4)	2.6 (0.2)	3.0 (0.1)
Rha	9.0 (0.4)	7.5 (0.0)	12.7 <sup>b</sup> (0.7)	10.2 <sup>c</sup> (0.4)	3.2 (0.3)	6.6 (0.2)	3.3 (0.7)	8.7 <sup>a</sup> (0.2)	2.3 (0.4)	9.8 (0.5)	2.7 (0.9)	14.2 <sup>a</sup> (0.4)	3.6 (0.6)	5.1 (0.4)	6.8 <sup>b</sup> (0.6)	7.9 <sup>a</sup> (0.0)
Ara	21.2 (1.2)	18.9 (1.9)	3.6 <sup>c</sup> (0.2)	2.7 <sup>c</sup> (0.0)	6.4 (0.8)	14.7 (1.0)	1.0 <sup>c</sup> (0.2)	2.8 <sup>c</sup> (0.0)	6.3 (1.9)	28.3 (2.5)	0.4 <sup>a</sup> (0.1)	2.5 <sup>c</sup> (0.1)	8.5 (1.0)	13.4 (0.5)	2.2 <sup>c</sup> (0.1)	2.8 <sup>c</sup> (0.1)
Gal	28.5 (1.4)	13.8 (0.8)	45.3 <sup>b</sup> (2.7)	23.2 <sup>a</sup> (2.0)	5.0 (0.4)	9.5 (0.2)	8.5 (2.4)	20.3 <sup>b</sup> (2.4)	5.5 (1.3)	20.9 (0.5)	5.2 (2.0)	25.4 (2.0)	18.1 (2.4)	23.8 (1.5)	31.5 <sup>b</sup> (3.6)	33.5 <sup>a</sup> (1.0)
Xyl	17.4 (0.5)	7.1 (0.3)	21.7 (0.9)	11.2 <sup>b</sup> (0.5)	2.2 (0.1)	4.9 (0.4)	2.6 (0.6)	7.5 <sup>b</sup> (0.4)	2.0 (0.3)	9.3 (0.9)	2.6 (0.5)	15.5 <sup>b</sup> (1.5)	13.2 (1.2)	21.0 (1.1)	16.5 (1.4)	21.1 (0.0)
GalA	70.1 (1.7)	50.8 (2.5)	66.0 (2.7)	50.0 (2.3)	38.9 (1.7)	63.1 (1.0)	28.7 (5.1)	59.0 (2.2)	9.3 (1.7)	30.4 (1.5)	9.7 (2.6)	40.6 <sup>a</sup> (0.9)	21.9 (1.8)	24.6 (1.7)	27.6 <sup>b</sup> (0.3)	25.1 (2.5)
GlcA	8.0 (0.5)	0.9 (0.1)	8.2 (0.9)	1.6 (0.4)	0.3 (0.0)	0.5 (0.0)	0.5 (0.1)	1.0 <sup>c</sup> (0.0)	0.2 (0.0)	0.5 (0.1)	0.3 (0.1)	1.1 <sup>b</sup> (0.0)	7.6 (1.6)	8.5 (1.9)	7.5 (2.7)	6.6 (1.9)

The values represent averages of three biological replicates (±SD).

<sup>a</sup>Significance at the 0.1% level.

<sup>b</sup>Significance at the 1% level.

<sup>c</sup>Significance at the 0.01% level.

when supplied with UDP-Arap. *Arabidopsis* has not been observed to produce arabinosylated xylan, which may explain why such interactions are not observed in this species. The mutase could be expected to be associated, for instance, with enzymes involved in arabinan biosynthesis, but if such direct interactions exist, they are not very strong. It has been observed that microsomes from potato and mung bean can incorporate arabinofuranose into polysaccharides with UDP-Arap as substrate, whereas isolated Golgi from these dicot species do not have this ability, consistent with a very loose association between RGP and Golgi in dicots (Nunan and Scheller, 2003; Konishi et al., 2006).

#### The Interconversion of UDP-Arap and UDP-Araf Is Indispensable for Plant Development

So far, only a few Ara-deficient mutants have been described. Potato plants expressing a Golgi-localized arabinanase have been reported to have about a 70% reduction in RG I arabinan content in potato tubers. Surprisingly, the plants did not show significant changes in total cell wall monosaccharide composition and did not reveal any phenotypic alterations compared with wild-type plants (Skjot et al., 2002). The *Arabidopsis arad1* mutant has been characterized with a 25 and 54% decrease in cell wall Ara in the leaf and stem, respectively. *ARAD1*, encoding a putative glycosyltransferase, is proposed to be involved in the biosynthesis of arabinan side chains of RG I, since changes in other Ara-containing polymers, including arabinogalactan and extensin proteins, were not observed (Harholt et al., 2006).

L-Ara residues in plant cell wall components have been mainly found in the furanose form rather than in the pyranose form,

which is thermodynamically more stable. We argue that the conversion of UDP-Arap into UDP-Araf is indispensable for plant cell wall synthesis, and a reduction in UDP-Arap mutase activity would consequently result in less Ara incorporated into plant cell wall polysaccharides. This hypothesis prompted us to investigate *Arabidopsis RGP1* and *RGP2* knockout mutants in detail.

*RGP1* and *RGP2* have previously been demonstrated to act redundantly in pollen development. Whereas single knockout mutants did not exhibit phenotypic alterations compared with wild-type plants, double knockouts were determined to be male gametophyte lethal, with an arrest in pollen mitosis (Drakakaki et al., 2006). However, single mutant lines were not analyzed with regard to cell wall monosaccharide composition in this study.

Consistent with Drakakaki et al. (2006), single knockout lines did not reveal any morphological alterations compared with the wild type. However, our cell wall monosaccharide analysis revealed significant 12 to 16% (*rgp1-1* and *rgp1-2*) and 30 to 31% (*rgp2-1* and *rgp2-2*) reductions in total leaf cell wall Ara content, which supports our hypothesis. Since double knockout lines have been shown to be gametophyte lethal (Drakakaki et al., 2006), we generated an RNA interference construct that specifically targets *RGP1* and *RGP2* expression. Subsequent monosaccharide analysis of leaf cell wall polysaccharides revealed an up to ~80% reduction in Ara content, correlating with the degree of suppression in *RGP1* and *RGP2* expression.

Cell wall fractionation studies indicated that the cell walls of hpRGP1/2 lines were not substantially altered, besides the decrease in Ara. However, the hpRGP1/2 walls had a disproportionate increase in Gal and Rha, indicating an increased RG I content. The RG I was less easily extracted. The change in sugars besides Ara is different from what has been observed in mutants

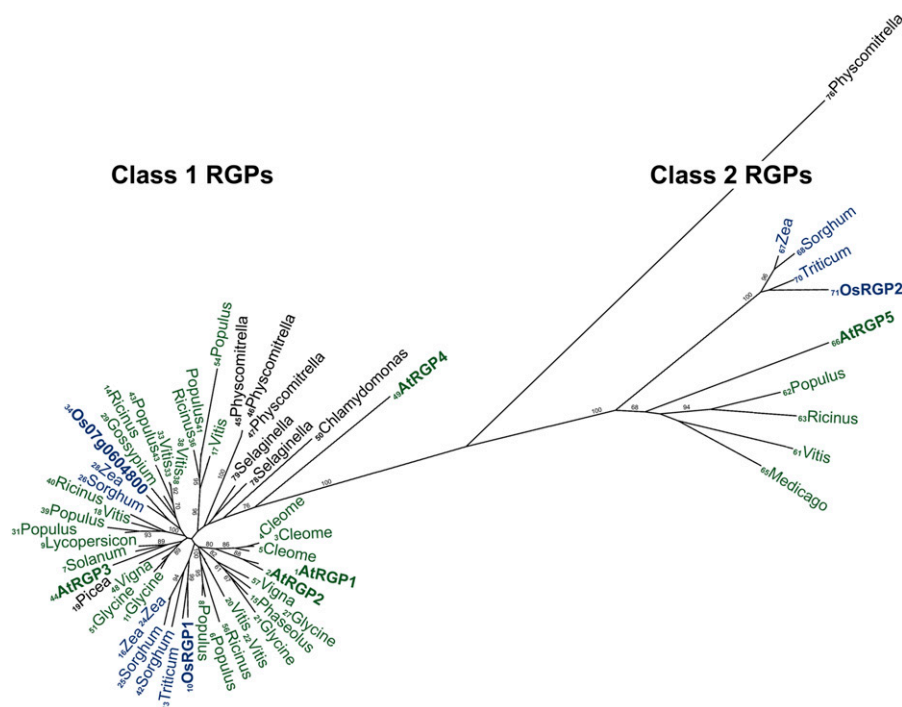


**Figure 7.** Bootstrapped Neighbor-Joining Tree of Plant RGP Full-Length Protein Sequences.

*Arabidopsis* RGPs are highlighted in boldface green and rice RGPs in boldface blue. Numbers at the nodes indicate bootstrap values calculated for 1000 replicates. Values of <60% were considered to be not significant and are not displayed. Based on experimental evidence and phylogenetic relationships, plant RGPs can be divided into mutases (class 1) and closely related proteins without mutase activity (class 2). [See online article for color version of this figure.]

and transformants specifically decreased in pectic arabinans (Skjøt et al., 2002; Harholt et al., 2006). However, the decrease in Ara in those studies was less dramatic than in our study.

Determination of UDP-Ara mutase activities in single *rgp1* and *rgp2* mutant lines revealed a significant reduction to ~50% of wild-type levels in cytosolic and microsomal protein extracts. In hpRGP1/2 lines, UDP-Ara mutase activity was barely detectable and was reduced to 1% of wild-type levels. Moreover, UDP-Ara contents were significantly higher in *rgp1* and *rgp2* mutants compared with the Col-0 wild-type, as was UDP-Xyl, the precursor for UDP-Ara synthesis. This suggests that strongly reducing the conversion of UDP-Ara to UDP-Araf and thus reducing the flux into cell wall polymers creates a bottleneck and a concomitant accumulation of immediate precursors.

Since *RGP1* and *RGP2* were strongly expressed in seed coat epidermal cells, the site of pectic mucilage production during seed development, we analyzed mucilage extrusion and solubility in the wild-type (EVC) and hpRGP1/2. L-Ara in arabinan side chains is a major constituent of pectin. In *Arabidopsis*, pectin mostly consists of the acidic polysaccharide RG I, which consists of repeats of the disaccharide ( $\rightarrow 4$ )- $\alpha$ -D-GalA-( $1 \rightarrow 2$ )- $\alpha$ -L-Rha-( $1 \rightarrow$ ). This backbone can be substituted with different types of side chains (arabinans, galactans, and type I arabinogalactans) on the Rha residues (Willats et al., 2001).

The seed coat secretory cells in *Arabidopsis* represent a useful model system for cell wall establishment, in particular for pectin

synthesis and modification (reviewed in Arsovski et al., 2010). During seed coat formation, the epidermal cells of *Arabidopsis* seeds synthesize and secrete large quantities of mucilage into the apoplast underneath the outer cell wall (Beeckman et al., 2000; Windsor et al., 2000). Upon imbibition, the mucilage is hydrated and released from the seed coat epidermis through rupture of the outer cell wall junctions. Among other factors, the number of side chains determine the swelling properties and solubility of the seed mucilage (Arsovski et al., 2009). An increase in ( $1 \rightarrow 4$ )- $\beta$ -galactan or ( $1 \rightarrow 5$ )- $\alpha$ -arabinan side chains negatively affects mucilage hydration properties and solubility (Dean et al., 2007; Macquet et al., 2007; Arsovski et al., 2009). Thus, a reduction in total cell wall Ara and consequently reduced ( $1 \rightarrow 5$ )- $\alpha$ -arabinan branches is expected to alter the hydration properties of the pectic seed mucilage and consequently increase its solubility. Ruthenium red stains of water-imbibed seeds derived from hpRGP1/2-7 and hpRGP1/2-9 lines with the greatest reduction in total cell wall Ara content indicated a rapid loss of the outer mucilage and only faint staining of the inner mucilage, whereas wild-type (EVC) seeds and seeds derived from other hpRGP1/2 lines with less of a reduction in Ara content (e.g., hpRGP1/2-1) showed intense staining of the outer mucilage as well as the inner mucilage, which was still attached to the seed. These observations, demonstrating that a reduction in Ara in general leads to an increased solubility of pectic mucilage, are consistent with and extend data that demonstrated that an

increase of arabinans or galactans caused by knockouts of a  $\alpha$ -L-arabinofuranosidase (Arsovski et al., 2009) or a  $\beta$ -galactosidase (Dean et al., 2007; Macquet et al., 2007), respectively, inhibits the proper expansion and solubilization of seed mucilage upon hydration.

The reduction of *RGP5* expression in hpAtRGP5 lines (up to ~85% compared with control plants) was not as strong as observed for *RGP1* and *RGP2* in hpRGP1/2 transgenic lines. However, despite having no effect on the obvious morphological phenotype, the similar levels of reduction in the expression of *RGP1* and *RGP2* in the hpRGP1/2-3, -4, and -8 lines were sufficient to cause a significant reduction in cell wall Ara content of ~40%. Thus, the biological function of RGP5 and the relevance of it being a consistent part of the RGP1/RGP2 protein complex remain elusive.

The substantial reduction in cell wall Ara and UDP-Ara mutase activity that resulted from downregulating RGP1 and RGP2 indicates that cytosolic RGPs constitute the only enzymes in *Arabidopsis* with UDP-Ara mutase activity. The main compartment for UDP-Arap synthesis is inside the Golgi vesicles, where UDP-Xyl (synthesized by UDP-Xyl synthase, which is also located inside the Golgi) is converted into UDP-Arap by UDP-Xyl-4-epimerase (Burget et al., 2003). Recently, some cytosolic UDP-Glc-4-epimerases, homologous with the Golgi-localized UDP-Xyl-4-epimerase, were shown to interconvert UDP-D-Xyl and UDP-L-Ara in vitro, providing evidence for a cytosolic de novo pathway for UDP-Ara generation (Kotake et al., 2009). However, given the strong effect on Ara content of inactivating one of the three UDP-Xyl-4-epimerases (Burget et al., 2003), it appears that the cytoplasmic route is of minor importance. There is another cytoplasmic pathway for the synthesis of UDP-Arap from free Ara by means of pyrophosphorylases. However, this pathway is a salvage pathway and uses Ara that was originally synthesized by UDP-Xyl-4-epimerase.

Virtually all of the Ara in the cell is used for cell wall biosynthesis, which also takes place inside the Golgi vesicles. It is therefore somewhat surprising that mutase activities are found in proteins that are present outside the Golgi lumen. The implication is that there must be transporters that transport UDP-Arap out of the Golgi and transporters (which could be different or the same) that transport UDP-Araf into the Golgi lumen.

## METHODS

### Plant Material and Plant Transformation

*Arabidopsis thaliana* Col-0 was obtained from the ABRC (<http://abrc.osu.edu/>). T-DNA insertion mutants *rgp2-1* (Salk\_132152) and *rgp2-2* (Salk\_148500) were localized in the SIGnAL Salk collection (<http://signal.salk.edu/>) and *rgp1-1* (GK-652F12) and *rgp1-2* (GK-844C11) in the GABI-Kat collection (<http://www.gabi-kat.de/>) and obtained from the ABRC. Plants were germinated and grown on soil (PRO-MIX; Premier Horticulture) in a growth chamber under short-day light conditions (10-h photoperiod [ $120 \mu\text{mol}\cdot\text{m}^{-2}\cdot\text{s}^{-1}$ ] at 22°C and 60% RH/14 h of dark at 22°C and 60% RH). After 4 weeks, plants were transferred to long-day conditions (16-h photoperiod [ $120 \mu\text{mol}\cdot\text{m}^{-2}\cdot\text{s}^{-1}$ ] at 22°C and 60% RH/8 h of dark at 22°C and 60% RH). *Arabidopsis* plants were transformed using *Agrobacterium tumefaciens* GV 3101 pmp90 as described by Clough and Bent (1998) via the floral dip method. For BASTA selection,

seeds were germinated on soil as described above and sprayed every 2 d for a total of five times with a glufosinate-ammonium (Crescent Chemical) solution (40  $\mu\text{g}/\text{mL}$ ). Resistant plants were transferred to new pots and further grown as described above. For kanamycin selection, seeds were germinated on half-concentrated Murashige and Skoog medium (Murashige and Skoog, 1962) supplemented with 1% (w/v) Suc, 75  $\mu\text{g}/\text{mL}$  kanamycin, and 100  $\mu\text{g}/\text{mL}$  cefotaxime (Sigma-Aldrich) and solidified with 0.7% (w/v) agar under a 16-h photoperiod ( $120 \mu\text{mol}\cdot\text{m}^{-2}\cdot\text{s}^{-1}$ , 22°C). After 10 d, plants were transferred to soil.

### Sequence Analysis

Amino acid sequences were retrieved by searching public databases using the BLAST algorithm (Altschul et al., 1990) at the National Center for Biotechnology Information (<http://www.ncbi.nlm.nih.gov/>). Deduced amino acid sequences were aligned using the ClustalX program (Thompson et al., 1997) with the default parameter. Phylogenetic trees were calculated using the MEGA application (Tamura et al., 2007) with the neighbor-joining method with bootstrap values generated from 1000 bootstrap samples. Only bootstrap values of >70% were considered to be significant (Hillis and Bull, 1993), and bootstrap values of <60% are not shown.

### Cloning Procedures

Sequenced, error-free open reading frame clones for *Arabidopsis RGP1* (U16497), *RGP2* (U12851), *RGP4* (U20586), and *RGP5* (U10383) were obtained from the Salk/Stanford/PGEN consortium (Yamada et al., 2003). *RGP3* was cloned from cDNA prepared from *Arabidopsis* siliques RNA. Sequences without a native stop codon were PCR amplified using the following primer pairs: RGP1-fwd (5'-CACCATGGTTGAGCCGGCGAACACCGTT-3') and RGP1-rev (5'-AGCTTTAGTGGGTGGGTTAAGCT-3'), RGP2-fwd (5'-CACCATGGTTGAGCCGGCGAATACT-3') and RGP2-rev (5'-AGCTTTGCCACTGGCTGCTGGT-3'), RGP3-fwd (5'-CACCATGGC-GCAATTGTATTCTTCC-3') and RGP3-rev (5'-ATTTTTGCCTTTTGGT-GCCTCAGCCT-3'), RGP4-fwd (5'-CACCATGGCGGGCTACAACCTC-GAAGTA-3') and RGP4-rev (5'-CTTGGCCTTGACATCTTTGCCA-3'), and RGP5-fwd (5'-CACCATGTCTTTGGCCGAGATAAACA-3') and RGP5-rev (5'-AGCGCTAGAATTAACAGAATTCC-3'). The resulting PCR products were introduced into the pENTR/SD/D-TOPO cloning vector (Invitrogen) according to the manufacturer's protocol, and their identities were verified by sequencing. For *Arabidopsis RGP* expression under the control of their native promoters as C-terminal translational HA tag or YFP-HA tag fusions, the corresponding promoter sequences (on average, the region 2 kb upstream of the ATG start codon) were PCR amplified from genomic DNA with *NotI* linker (lowercase letters) using RGP1pro-fwd (5'-ttgcgccgcaaTTGATCTTGACGCCGCTTTG-3') and RGP1pro-rev (5'-ttgcgccgcaaGATTGGATTGATTCAGAGAGAAGAGAA-3'), RGP2pro-fwd (5'-ttgcgccgcaaTGATCATTCTCATTGATGCTGTGTCTC-3') and RGP2pro-rev (5'-ttgcgccgcaaGTTTTCGAAATGAGAGAGATGAGATGATCG-3'), RGP3pro-fwd (5'-ttgcgccgcaaCGCAAACCTCGCCATGAGTGG-3') and RGP3pro-rev (5'-ttgcgccgcaaTTGAAACGACAAGGAAGAAAGA-3'), RGP4pro-fwd (5'-ttgcgccgcaaCGAAACCTAAAATTGAACCCGTC-3') and RGP4pro-rev (5'-ttgcgccgcaaTTTGGTACTTAAAGTTAATTAGATGTGTA-3'), and RGP5pro-fwd (5'-ttgcgccgcaaTCTTCGGATTGTGAAATCAGATCG-3') and RGP5pro-rev (5'-ttgcgccgcaaTTCGAGTTTCAACAATCTTTAAGCA-3'). Following restriction digestion, promoter sequences were ligated into the *NotI* site of the pENTR/SD/D-TOPO cloning vector upstream of the corresponding *RGP* coding sequence. Orientations and identities were verified by sequencing. To obtain HA tag fusions, the constructs were introduced into the promoterless pEarleyGate301 plant transformation vector (Earley et al., 2006) using LR clonase (Invitrogen) according to the manufacturer's protocol. C-terminal YFP-HA tag fusion constructs were generated by

replacing the *NcoI/MunI* cassette from pEarleyGate301 with the *NcoI/MunI* cassette derived from pEarleyGate101. Hairpin constructs, either directed against *RGP1* and *RGP2* or *RGP5*, were assembled as described by Wesley et al. (2001) and named hpRGP1/2 and hpRGP5, respectively. Fragments of 299 and 485 bp were amplified from cDNA using the following primer pairs: hpRGP1/2s-fwd (5'-acggaattccgGGATCCATCTGGAAAAGCTGTGA-3') and hpRGP1/2s-rev (5'-ggggtaccacTACCACACATAGGGAAAAGAGTTCC-3'), hpRGP1/2as-fwd (5'-a gctctagagcGGATCCATCTGGAAAAGCTGTGA-3') and hpRGP1/2as-rev (5'-ccatcgatggTACCACACATAGGGAAAAGAGTTCC-3'), hpRGP5s-fwd (5'-acggaattccgTATAATTTTGTGGTATTGCTTG-3') and hpRGP5s-rev (5'-ggggtaccacTGAGTAACAGCATCCACTAGGAACC-3'), and hpRGP5as-fwd (5'-agctctagagcTATAATTTTGTGGTATTGCTTG-3') and hpRGP5as-rev (5'-ccatcgatggTGAGTAACAGCATCCACTAGGAACC-3'), digested with either *EcoRI* and *KpnI* or *XbaI* and *Clal*, sequentially cloned into the pHANNIBAL vector, and subsequently subcloned into the plant transformation vector pART27 as a *NotI* cassette. For heterologous expression in *Escherichia coli*, coding sequences without a native stop codon were recombined into the pET-DEST42 bacterial expression vector (Invitrogen), which introduces a C-terminal V5 epitope and hexahistidine tags, using LR clonase (Invitrogen), according to the manufacturer's protocol. For stable and transient expression of RGP-YFP fusion proteins driven by the constitutive CaMV 35S promoter, coding sequences without a native stop codon were recombined into the pEarleyGate101 plant expression vector. Transient expression in tobacco (*Nicotiana benthamiana*) was performed as described by Jensen et al. (2008).

#### Heterologous Expression and Enzyme Purification

The respective constructs were introduced into BL-21 Star (DE3) chemically competent *E. coli* (Invitrogen), according to the manufacturer's instructions. Single bacterial colonies, grown on Luria-Bertani agar containing 100  $\mu\text{g}/\text{mL}$  carbenicillin, were isolated, used to inoculate 5-mL liquid cultures supplemented with 100  $\mu\text{g}/\text{mL}$  carbenicillin, and grown overnight at 37°C. The overnight cultures were used to inoculate 0.2 liters of Luria-Bertani cultures containing 100  $\mu\text{g}/\text{mL}$  carbenicillin, which were grown at 37°C until OD<sub>600</sub> reached  $\sim 0.3$ . Expression was induced by the addition of 1 mM isopropyl- $\beta$ -D-thiogalactopyranoside, and the cultures were further grown at 20°C overnight. Recombinant proteins were affinity purified using a HIS-Select HF Nickel Affinity gel (Sigma-Aldrich) according to the manufacturer's instructions and desalted with PD-10 desalting columns (GE Healthcare). Purity and integrity were verified by SDS-PAGE, and the recombinant proteins were stored at  $-20^\circ\text{C}$  in 20 mM Tris buffer, pH 7.5, containing 20% (v/v) glycerol.

#### Enzyme Activity Assay

UDP-Arap was obtained from Carbosource Service and UDP-Araf (triethanolamine salt) from the Peptide Research Institute. UDP-Ara mutase assays were performed at 30°C for 1 h (providing UDP-Arap as substrate) or 10 min (using UDP-Araf as substrate) in 20 mM Tris buffer, pH 6.8, 5 mM MnCl<sub>2</sub> containing 1 nmol of UDP-Arap or UDP-Araf and 200 ng of recombinant plant proteins, 200 ng of immunoprecipitated protein complex, or 40  $\mu\text{g}$  of fractionated plant proteins. The reaction was terminated by adding 9 volumes of ethanol (99%) and subjected to high-performance anion-exchange chromatography (HPAEC). HPAEC analysis was performed using a Dionex Ultimate 3000 apparatus with UV light detection at 262 nm. Samples were separated on a CarboPac PA20 column (3  $\times$  150 mm; Dionex). Prior to injection (20  $\mu\text{L}$ ), the samples were spin filtered (0.45  $\mu\text{m}$ ). A flow of 0.5 mL/min and a linear gradient of 50 mM to 1 M ammonium formate was applied as follows: 0 to 2.1 min, 50 mM, isocratic;

2.1 to 40 min, 50 mM to 1 M, linear; 40 to 45 min, 1 M to 50 mM, linear; 45 to 55 min, 50 mM, isocratic. The formation of UDP-Arap and UDP-Araf was confirmed by LC-ESI-MS, as described by Konishi et al. (2007), using a TSQ Quantum Discovery Max mass spectrometer (Thermo Fisher Scientific) and a Synergy Hydro-RP 4u 160  $\times$  2.5 mm column (Phenomenex) operated with a flow of 0.25 mL/min.

#### Determination of Nucleotide Sugars

After grinding plants to a fine powder and performing metabolite extraction (Arrivault et al., 2009) and Carbo column purification, nucleotide sugars were determined by ion-pair chromatography-MS/MS analysis (T. Herter, S. Arrivault, S. Osorio, A. Schlereth, D. Pese, B. Arsova, P. Troc, S. Endres, R. Tenhaken, C. Rautengarten, S.M. Bulley, H.V. Scheller, M. Stitt, A.R. Fernie, S. Kempa, W.D. Reiter, and B. Usadel, unpublished data). In brief, chromatography was performed on a Dionex Ultimate 3000 HPLC system using a reverse-phase Synergi 4u Hydro 80A 150  $\times$  2.0 mm column at a temperature of 28°C. A flow of 0.25 mL/min and a gradient of acetonitrile in 20 mM buffered triethylamine/acetic acid, pH 6.0, was established as follows: 0 to 15 min, 0% acetonitrile, isocratic; 15 to 35 min, 0 to 3.5% acetonitrile, linear; 35 to 45 min, 3.5 to 90% acetonitrile, linear; 45 to 48 min, 90% acetonitrile, isocratic; 48 to 59 min, 90 to 0% acetonitrile, linear. Detection relied on a Thermo-Finnigan TSQ Quantum Discovery triple quadrupole mass spectrometer (Thermo Scientific) equipped with an electrospray interface in negative ion mode with selected reaction monitoring.

#### Protein Extraction, Immunoblotting, and Immunoprecipitation

Plant material was ground in liquid nitrogen. Total protein was extracted in 1 volume (v/w) of immunoprecipitation buffer (150 mM NaCl, 10 mM Tris, pH 8.0) supplemented with various detergent concentrations (0.1–2% Nonidet P-40 substitute; Sigma-Aldrich). The resulting homogenate was thoroughly shaken for 30 min at 4°C and centrifuged at 20,800g at 4°C for 10 min, and the supernatant was collected. Protein concentrations were determined according to Bradford (1976). For immunoblot analysis, protein extracts were resolved by SDS-PAGE on 7 to 15% gradient gels and blotted onto nitrocellulose membranes (GE Healthcare). Blots were probed with a 1:1000 dilution of rabbit anti-cFBPase, anti-Sar1 (Agrisera; AS04 043 and AS08 326) or anti-calreticulin (Abcam; ab2907), or a 1:10,000 dilution of rabbit anti-HA or mouse anti-polyhistidine antibody, respectively (Sigma-Aldrich), followed by a 1:20,000 dilution of goat anti-rabbit or goat anti-mouse IgG conjugated to horseradish peroxidase (Sigma-Aldrich), before applying ECL Plus detection reagent (GE Healthcare). Blots were imaged using a ChemiDoc-Iit 600 Imaging System (UVP), and images were processed in Adobe Photoshop (Adobe Systems). For immunoprecipitations, 5 to 10 mg of total protein was incubated with 5  $\mu\text{g}$  of anti-HA antibody at 4°C on a rotary shaker. After 3 h, 75  $\mu\text{L}$  of protein A-Sepharose (Sigma-Aldrich) was added, and the sample was incubated for an additional 1 h. After centrifugation at 8000g for 10 s, the supernatant was removed and the sample was washed three times with immunoprecipitation buffer and 0.1% (v/v) Nonidet P-40 and three times with 10 mM Tris, pH 8.0. Protein was eluted with 500  $\mu\text{L}$  of 10 mM Tris, pH 8.0, containing 100  $\mu\text{g}$  of HA peptide (Sigma-Aldrich), and concentrated using Vivaspin sample concentrators (GE Healthcare). Aliquots were separated by SDS-PAGE, and gels were blotted onto nitrocellulose membranes as described above or stained with Sypro Ruby protein gel stain (Invitrogen), according to the manufacturer's protocol. For LC-ESI-MS/MS, immunoprecipitation samples were dried in a Speedvac and resuspended in 50  $\mu\text{L}$  of 25 mM NH<sub>4</sub>CO<sub>3</sub>/40% (v/v) methanol. Then, 2  $\mu\text{L}$  of 100 mM DTT was added, and the samples were heated for 5 min at 95°C. A total of 0.5  $\mu\text{g}$  of MS-grade trypsin (Invitrogen) was added, and the sample was digested for 16 h at 37°C. Peptide

mixtures were dried in a Speedvac and resuspended in 50  $\mu$ L of 0.5% (v/v) trifluoroacetic acid/5% (v/v) acetonitrile. Samples were desalted with PepClean C-18 Spin columns (Pierce), according to the manufacturer's instructions.

### Microsome Preparation and Subcellular Protein Fractionation

Ground plant material was resuspended in 1 mL of extraction buffer (5 mM sodium phosphate, pH 7.1, 400 mM Suc, and 1 mM DTT). The suspension was filtered through two layers of Miracloth and centrifuged for 10 min at 3000g at 4°C. The supernatant was centrifuged at 50,000g at 4°C for 1 h. The resulting supernatant (F1), containing cytosolic proteins, was removed. The remaining pellet was washed with 1 mL of extraction buffer and centrifuged as above. Peripherally attached membrane proteins were stripped with 400  $\mu$ L of 100 mM Na<sub>2</sub>CO<sub>3</sub>, pH 11.5, for 30 min on ice (Fujiki et al., 1982). The procedure was repeated, and the supernatants were combined. The membrane pellet was resuspended in 400  $\mu$ L of 10 mM Tris, pH 7.5, 10% (v/v) glycerol, and 1 mM DTT and solubilized with 0.4% (v/v) Triton X-100 for 30 min on ice. Proteinase K protection assays of microsomal fractions were performed in 500  $\mu$ L of 50 mM Tris, pH 7.5, 5 mM CaCl<sub>2</sub>, and 10% (v/v) glycerol supplemented with 100  $\mu$ g of proteinase K (Invitrogen) for 1 h at 22°C. The reaction was terminated by the addition of 5 mM phenylmethylsulfonyl fluoride, and membranes were solubilized as described above. Fractions were concentrated using Vivaspin sample concentrators for further analysis (GE Healthcare).

### Quadrupole Time-of-Flight MS

Peptide mixtures were injected onto a Pepmap100  $\mu$ -guard column (Dionex) via Tempo Nano Autosampler and washed for 20 min. Peptides were separated on a Dionex Pepmap100 analytical column (75  $\mu$ m i.d., 150 mm length, 100 Å, 3  $\mu$ m) by using a TEMPO nanoLC-2D (Applied Biosystems) LC system coupled to a nano-ESI source operating in positive ion mode (2300–2400 V). LC conditions consisted of a 7-min wash period with buffer A (2% [v/v] acetonitrile, 0.1% [v/v] formic acid), followed by peptide elution with a gradient of 5 to 35% buffer B (98% [v/v] acetonitrile, 0.1% [v/v] formic acid) over 30 min, and a ramp from 35 to 80% (v/v) buffer B over 5 min. The conditions were maintained at 80% (v/v) buffer B for 15 min followed by column reequilibration by a decreasing gradient of buffer B of 80 to 5% (v/v), in 5 min, and held for 15 min. Mass analysis was performed using a QSTAR Elite mass spectrometer (Applied Biosystems) operating in information-dependent acquisition mode consisting of one MS scan (350–1600 D) followed by up to three product ion scans (100–1600 D). A precursor ion signal of >30 counts was required before MS/MS fragmentation was triggered. The product ion scans were collected from each cycle with a maximum accumulation time of 2 s (fragment multiplier = 4), depending on the intensities of the fragment ions. Parent ions (mass tolerance = 100 ppm) and their isotopes were excluded from further selection for 1 min.

### MS Data Analysis

Mascot Distiller (version 2.1) was used to sum similar precursor ion scans from each LC-MS/MS run and to generate product ion peak lists for subsequent database searches. A Mascot MS/MS Ion Search (Mascot version 2.2.04; MatrixScience) was performed for each data set against a protein database consisting of all putative open reading frame sequences of *Arabidopsis* (TAIR9) appended with trypsin, BSA, and common contaminants (33,417 total sequences). Only fully digested peptides with up to one missed cleavage site were considered, and oxidation of Met was considered as a variable modification. Precursor and product ion tolerances were set at  $\pm$ 100 ppm and  $\pm$ 0.3 D, respectively.

### Microscopy

Tissue samples were mounted in 10% (v/v) glycerol or 20 mM sodium phosphate buffer, pH 7.1, containing 10  $\mu$ g/mL propidium iodide. Images were collected using a Leica MZ16F fluorescence stereomicroscope with 470 or 360 nm for GFP or UV light excitation, respectively. Confocal laser scanning microscopy was performed using a Zeiss LSM 710 device equipped with an argon laser (514 nm for YFP excitation) and an In Tune laser (536 nm for propidium iodide excitation; Zeiss). Emission was collected at 510 to 545 nm (YFP) and 610 to 650 nm (propidium iodide). The pinhole diameter was set at 1 airy unit. Images were processed in ImageJ 1.42q (<http://rsb.info.nih.gov/ij>) and Adobe Photoshop (Adobe Systems). Seed mucilage was stained as described previously (Rautengarten et al., 2008).

### Cell Wall Preparation and Determination of Monosaccharide Composition

Alcohol insoluble residue was prepared as described earlier (Harholt et al., 2006). Alcohol insoluble residue was sequentially extracted with 50 mM CDTA for 2 h at 4°C, 50 mM CDTA for 16 h at 4°C, 50 mM Na<sub>2</sub>CO<sub>3</sub> containing 20 mg/mL NaBH<sub>4</sub> for 2 h at 4°C, and 50 mM Na<sub>2</sub>CO<sub>3</sub> containing 20 mg/mL NaBH<sub>4</sub> for 16 h at 4°C. CDTA fractions were combined and dialyzed against 50 mM sodium acetate, pH 5.5, overnight at 4°C, followed by three changes of water. Sodium carbonate fractions were combined, neutralized with acetic acid, and dialyzed against three changes of water. Fractions were freeze-dried. The insoluble residue was washed with water, 70% (v/v) ethanol, and acetone and dried. Total alcohol insoluble residue or corresponding fractions were hydrolyzed in 2 N trifluoroacetic acid for 1 h at 120°C. HPAEC with pulsed amperometric detection was performed according to Øbro et al. (2004) on a ICS 3000 device (Dionex) using a CarboPac PA20 (3  $\times$  150 mm) anion-exchange column (Dionex). The results were analyzed by two-way and three-way ANOVA.

### RT-PCR

RNA was extracted using the RNEasy RNA Plant kit (Qiagen), according to the manufacturer's protocol. One microgram of total RNA was reverse transcribed with SuperScriptII reverse transcriptase and d(T)<sub>15</sub> oligomers (Invitrogen), according to the manufacturer's protocol. Real-time PCR was performed with Absolute SYBR Green ROX mix (ABgene) on a StepOnePlus real-time PCR system (Applied Biosystems), according to previously described conditions (Czechowski et al., 2005), using StepOne 2.0 software (Applied Biosystems). *Arabidopsis* *RGP1* was amplified using 5'-CAGGAACGACATCAACCGTA-3' (fwd) and 5'-TGGATCCT-TAGCAACGAAGC-3' (rev), *RGP2* was amplified using 5'-GAACGACAT-TAACGGAATCCTC-3' (fwd) and 5'-GATCCTTGGAACGAAGC-3' (rev), *RGP3* was amplified using 5'-AATACGAAATCGCTTACGATAAGTCT-3' (fwd) and 5'-CATCGCTCCAGTCATAGGC-3' (rev), *RGP4* was amplified using 5'-AGATGGAAGTATTTCGTGAGAG-3' (fwd) and 5'-TCCACA-TACCTCGTGTACGTTTC-3' (rev), and *RGP5* was amplified using 5'-TGACATGGAAAAGGTTGTGG-3' (fwd) and 5'-ATCCACTAGGAAC-CCCTTCG-3' (rev). As a reference, primers for UBQ10, 5'-GGCCTTGTA-TAATCCCTGATGAATAAG-3' (fwd) and 5'-AAAGAGATAACAGGAACG-GAAACATAGT-3' (rev), were used.

### Accession Numbers

Sequence data from this article can be found in the Arabidopsis Genome Initiative or GenBank/EMBL databases under the accession numbers listed in Supplemental Table 4 online.

### Supplemental Data

The following materials are available in the online version of this article.

**Supplemental Figure 1.** UDP-Ara Mutase Activities of Immunoprecipitated RGP-YFP Fusion Proteins.

**Supplemental Figure 2.** Complementation of RGP Mutant Lines by HA and YFP Tag Fusion Proteins.

**Supplemental Figure 3.** Subcellular Localizations of RGPs When Stably Expressed as C-Terminal YFP Fusion Proteins Driven by the Constitutive CaMV 35S Promoter in *Arabidopsis*.

**Supplemental Figure 4.** Subcellular Localizations of RGPs When Transiently Expressed as C-Terminal YFP Fusion Proteins Driven by the Constitutive CaMV 35S Promoter in Tobacco Leaves.

**Supplemental Figure 5.** Mutase Activities of RGP Complexes Determined Using UDP-Arap as Substrate.

**Supplemental Figure 6.** qRT-PCR Analysis of RGP5 Expression in hpRGP5 Lines.

**Supplemental Table 1.** Peptide Sequences of Identified RGP Complex Components.

**Supplemental Table 2.** Monosaccharide Composition of Leaf Cell Wall Polysaccharides Extracted from the Wild Type (Col-0), *atrgp1*, and *atrgp2* Mutants.

**Supplemental Table 3.** Monosaccharide Composition of Polysaccharides Extracted from Leaf Material of hpRGP1/2 and hpRGP5 Transgenic Plants.

**Supplemental Table 4.** RGP Protein Accession Numbers and Annotations.

**Supplemental Data Set 1.** Multiple Sequence Alignment of 60 Nonredundant RGP Full-Length Protein Sequences.

## ACKNOWLEDGMENTS

Sherry Chan is thanked for assistance with plant growth. We thank the Commonwealth Scientific and Industrial Research Organization for providing the pHANNIBAL and pART27 vectors that were used for silencing of *AtRGP1/2* and *AtRGP5*. This work was supported by the U.S. Department of Energy, Office of Science, Office of Biological and Environmental Research, through contract DE-AC02-05CH11231 between the Lawrence Berkeley National Laboratory and the U.S. Department of Energy.

Received January 31, 2011; revised March 10, 2011; accepted March 23, 2011; published April 8, 2011.

## REFERENCES

- Alonso, J.M., et al. (2003). Genome-wide insertional mutagenesis of *Arabidopsis thaliana*. *Science* **301**: 653–657.
- Altschul, S.F., Gish, W., Miller, W., Myers, E.W., and Lipman, D.J. (1990). Basic local alignment search tool. *J. Mol. Biol.* **215**: 403–410.
- Arrivault, S., Guenther, M., Ivakov, A., Feil, R., Vosloh, D., van Dongen, J.T., Sulpice, R., and Stitt, M. (2009). Use of reverse-phase liquid chromatography, linked to tandem mass spectrometry, to profile the Calvin cycle and other metabolic intermediates in *Arabidopsis* rosettes at different carbon dioxide concentrations. *Plant J.* **59**: 826–839.
- Arsovski, A.A., Haughn, G.W., and Western, T.L. (2010). Seed coat mucilage cells of *Arabidopsis thaliana* as a model for plant cell wall research. *Plant Signal. Behav.* **5**: 796–801.
- Arsovski, A.A., Popma, T.M., Haughn, G.W., Carpita, N.C., McCann, M.C., and Western, T.L. (2009). *AtBXL1* encodes a bifunctional  $\beta$ -D-xylosidase/ $\alpha$ -L-arabinofuranosidase required for pectic arabinan modification in *Arabidopsis* mucilage secretory cells. *Plant Physiol.* **150**: 1219–1234.
- Beeckman, T., De Rycke, R., Viane, R., and Inze, D. (2000). Histological study of seed coat development in *Arabidopsis thaliana*. *J. Plant Res.* **113**: 139–148.
- Bocca, S.N., Kissen, R., Rojas-Beltrán, J.A., Noël, F., Gebhardt, C., Moreno, S., du Jardin, P., and Tandecarz, J.S. (1999). Molecular cloning and characterization of the enzyme UDP-glucose:protein transglucosylase from potato. *Plant Physiol. Biochem.* **37**: 809–819.
- Bradford, M.M. (1976). A rapid and sensitive method for the quantitation of microgram quantities of protein utilizing the principle of protein-dye binding. *Anal. Biochem.* **72**: 248–254.
- Burget, E.G., Verma, R., Mølhøj, M., and Reiter, W.D. (2003). The biosynthesis of L-arabinose in plants: Molecular cloning and characterization of a Golgi-localized UDP-D-xylose 4-epimerase encoded by the MUR4 gene of *Arabidopsis*. *Plant Cell* **15**: 523–531.
- Christensen, A., et al. (2010). Higher plant calreticulins have acquired specialized functions in *Arabidopsis*. *PLoS ONE* **5**: e11342.
- Clough, S.J., and Bent, A.F. (1998). Floral dip: A simplified method for *Agrobacterium*-mediated transformation of *Arabidopsis thaliana*. *Plant J.* **16**: 735–743.
- Czechowski, T., Stitt, M., Altmann, T., Udvardi, M.K., and Scheible, W.R. (2005). Genome-wide identification and testing of superior reference genes for transcript normalization in *Arabidopsis*. *Plant Physiol.* **139**: 5–17.
- Dean, G.H., Zheng, H., Tewari, J., Huang, J., Young, D.S., Hwang, Y.T., Western, T.L., Carpita, N.C., McCann, M.C., Mansfield, S.D., and Haughn, G.W. (2007). The *Arabidopsis* MUM2 gene encodes a  $\beta$ -galactosidase required for the production of seed coat mucilage with correct hydration properties. *Plant Cell* **19**: 4007–4021.
- Delgado, I.J., Wang, Z., de Rocher, A., Keegstra, K., and Raikhel, N.V. (1998). Cloning and characterization of AtRGP1. A reversibly autoglycosylated *Arabidopsis* protein implicated in cell wall biosynthesis. *Plant Physiol.* **116**: 1339–1350.
- De Pino, V., Borán, M., Norambuena, L., González, M., Reyes, F., Orellana, A., and Moreno, S. (2007). Complex formation regulates the glycosylation of the reversibly glycosylated polypeptide. *Planta* **226**: 335–345.
- De Smet, I., Lau, S., Mayer, U., and Jürgens, G. (2010). Embryogenesis—The humble beginnings of plant life. *Plant J.* **61**: 959–970.
- Dhugga, K.S., Tiwari, S.C., and Ray, P.M. (1997). A reversibly glycosylated polypeptide (RGP1) possibly involved in plant cell wall synthesis: Purification, gene cloning, and trans-Golgi localization. *Proc. Natl. Acad. Sci. USA* **94**: 7679–7684.
- Dhugga, K.S., Ulvskov, P., Gallagher, S.R., and Ray, P.M. (1991). Plant polypeptides reversibly glycosylated by UDP-glucose. Possible components of Golgi beta-glucan synthase in pea cells. *J. Biol. Chem.* **266**: 21977–21984.
- Drakakaki, G., Zabolina, O., Delgado, I., Robert, S., Keegstra, K., and Raikhel, N.V. (2006). *Arabidopsis* reversibly glycosylated polypeptides 1 and 2 are essential for pollen development. *Plant Physiol.* **142**: 1480–1492.
- Dry, I., Smith, A., Edwards, A., Bhattacharyya, M., Dunn, P., and Martin, C. (1992). Characterization of cDNAs encoding two isoforms of granule-bound starch synthase which show differential expression in developing storage organs of pea and potato. *Plant J.* **2**: 193–202.
- Earley, K.W., Haag, J.R., Pontes, O., Opper, K., Juehne, T., Song, K., and Pikaard, C.S. (2006). Gateway-compatible vectors for plant functional genomics and proteomics. *Plant J.* **45**: 616–629.



- Fettke, J., Eckermann, N., Tiessen, A., Geigenberger, P., and Steup, M.** (2005). Identification, subcellular localization and biochemical characterization of water-soluble heteroglycans (SHG) in leaves of *Arabidopsis thaliana* L.: Distinct SHG reside in the cytosol and in the apoplast. *Plant J.* **43**: 568–585.
- Fujiki, Y., Hubbard, A.L., Fowler, S., and Lazarow, P.B.** (1982). Isolation of intracellular membranes by means of sodium carbonate treatment: Application to endoplasmic reticulum. *J. Cell Biol.* **93**: 97–102.
- Gomez, L.D., Steele-King, C.G., Jones, L., Foster, J.M., Vuttipongchaikij, S., and McQueen-Mason, S.J.** (2009). Arabinan metabolism during seed development and germination in *Arabidopsis*. *Mol Plant* **2**: 966–976.
- Hanke, D.E., and Northcote, D.H.** (1975). Molecular visualization of pectin and DNA by ruthenium red. *Biopolymers* **14**: 1–17.
- Harholt, J., Jensen, J.K., Sørensen, S.O., Orfila, C., Pauly, M., and Scheller, H.V.** (2006). ARABINAN DEFICIENT 1 is a putative arabinosyltransferase involved in biosynthesis of pectic arabinan in *Arabidopsis*. *Plant Physiol.* **140**: 49–58.
- Hillis, D., and Bull, J.** (1993). An empirical test of bootstrapping as a method for assessing confidence in phylogenetic trees. *Syst. Biol.* **42**: 182–192.
- Jensen, J.K., et al.** (2008). Identification of a xylogalacturonan xylosyltransferase involved in pectin biosynthesis in *Arabidopsis*. *Plant Cell* **20**: 1289–1302.
- Jia, X.Y., He, L.H., Jing, R.L., and Li, R.Z.** (2009). Calreticulin: Conserved protein and diverse functions in plants. *Physiol. Plant.* **136**: 127–138.
- Konishi, T., Miyazaki, Y., Yamakawa, S., Iwai, H., Satoh, S., and Ishii, T.** (2010). Purification and biochemical characterization of recombinant rice UDP-arabinopyranose mutase generated in insect cells. *Biosci. Biotechnol. Biochem.* **74**: 191–194.
- Konishi, T., Ono, H., Ohnishi-Kameyama, M., Kaneko, S., and Ishii, T.** (2006). Identification of a mung bean arabinofuranosyltransferase that transfers arabinofuranosyl residues onto (1,5)-linked  $\alpha$ -L-arabinooligosaccharides. *Plant Physiol.* **141**: 1098–1105.
- Konishi, T., Takeda, T., Miyazaki, Y., Ohnishi-Kameyama, M., Hayashi, T., O'Neill, M.A., and Ishii, T.** (2007). A plant mutase that interconverts UDP-arabinofuranose and UDP-arabinopyranose. *Glycobiology* **17**: 345–354.
- Kotake, T., Takata, R., Verma, R., Takaba, M., Yamaguchi, D., Orita, T., Kaneko, S., Matsuoka, K., Koyama, T., Reiter, W.D., and Tsumuraya, Y.** (2009). Bifunctional cytosolic UDP-glucose 4-epimerases catalyze the interconversion between UDP-D-xylose and UDP-L-arabinose in plants. *Biochem. J.* **424**: 169–177.
- Langeveld, S.M., Vennik, M., Kottenhagen, M., Van Wijk, R., Buijk, A., Kijne, J.W., and de Pater, S.** (2002). Glucosylation activity and complex formation of two classes of reversibly glycosylated polypeptides. *Plant Physiol.* **129**: 278–289.
- Le, B.H., et al.** (2010). Global analysis of gene activity during *Arabidopsis* seed development and identification of seed-specific transcription factors. *Proc. Natl. Acad. Sci. USA* **107**: 8063–8070.
- Macquet, A., Ralet, M.C., Loudet, O., Kronenberger, J., Mouille, G., Marion-Poll, A., and North, H.M.** (2007). A naturally occurring mutation in an *Arabidopsis* accession affects a  $\beta$ -D-galactosidase that increases the hydrophilic potential of rhamnogalacturonan I in seed mucilage. *Plant Cell* **19**: 3990–4006.
- Memon, A.R.** (2004). The role of ADP-ribosylation factor and SAR1 in vesicular trafficking in plants. *Biochim. Biophys. Acta* **1664**: 9–30.
- Mohnen, D.** (2008). Pectin structure and biosynthesis. *Curr. Opin. Plant Biol.* **11**: 266–277.
- Munro, S., and Pelham, H.R.** (1987). A C-terminal signal prevents secretion of luminal ER proteins. *Cell* **48**: 899–907.
- Murashige, T., and Skoog, F.** (1962). A revised medium for rapid growth and bioassays with tobacco tissue cultures. *Physiol. Plant.* **15**: 473–497.
- Nunan, K.J., and Scheller, H.V.** (2003). Solubilization of an arabinan arabinosyltransferase activity from mung bean hypocotyls. *Plant Physiol.* **132**: 331–342.
- Øbro, J., Harholt, J., Scheller, H.V., and Orfila, C.** (2004). Rhamnogalacturonan I in *Solanum tuberosum* tubers contains complex arabinogalactan structures. *Phytochemistry* **65**: 1429–1438.
- Porchia, A.C., Sørensen, S.O., and Scheller, H.V.** (2002). Arabinoxylan biosynthesis in wheat. Characterization of arabinosyltransferase activity in Golgi membranes. *Plant Physiol.* **130**: 432–441.
- Rautengarten, C., Usadel, B., Neumetzler, L., Hartmann, J., Büssis, D., and Altmann, T.** (2008). A subtilisin-like serine protease essential for mucilage release from *Arabidopsis* seed coats. *Plant J.* **54**: 466–480.
- Rosso, M.G., Li, Y., Strizhov, N., Reiss, B., Dekker, K., and Weisshaar, B.** (2003). An *Arabidopsis thaliana* T-DNA mutagenized population (GABI-Kat) for flanking sequence tag-based reverse genetics. *Plant Mol. Biol.* **53**: 247–259.
- Rothschild, A., Wald, F.A., Bocca, S.N., and Tandecarz, J.S.** (1996). Inhibition of UDP-glucose:protein transglucosylase by a maize endosperm protein factor. *Cell. Mol. Biol. (Noisy-le-grand)* **42**: 645–651.
- Sagi, G., Katz, A., Guenoune-Gelbart, D., and Epel, B.L.** (2005). Class 1 reversibly glycosylated polypeptides are plasmodesmal-associated proteins delivered to plasmodesmata via the Golgi apparatus. *Plant Cell* **17**: 1788–1800.
- Scheller, H.V., and Ulvskov, P.** (2010). Hemicelluloses. *Annu. Rev. Plant Biol.* **61**: 263–289.
- Selth, L.A., Dogra, S.C., Rasheed, M.S., Randles, J.W., and Rezaian, M.A.** (2006). Identification and characterization of a host reversibly glycosylated peptide that interacts with the tomato leaf curl virus V1 protein. *Plant Mol. Biol.* **61**: 297–310.
- Singh, D.G., Lomako, J., Lomako, W.M., Whelan, W.J., Meyer, H.E., Serwe, M., and Metzger, J.W.** (1995).  $\beta$ -Glucosylarginine: A new glucose-protein bond in a self-glucosylating protein from sweet corn. *FEBS Lett.* **376**: 61–64.
- Skjøt, M., Pauly, M., Bush, M.S., Borkhardt, B., McCann, M.C., and Ulvskov, P.** (2002). Direct interference with rhamnogalacturonan I biosynthesis in Golgi vesicles. *Plant Physiol.* **129**: 95–102.
- Strand, A., Zrenner, R., Trevanion, S., Stitt, M., Gustafsson, P., and Gardeström, P.** (2000). Decreased expression of two key enzymes in the sucrose biosynthesis pathway, cytosolic fructose-1,6-bisphosphatase and sucrose phosphate synthase, has remarkably different consequences for photosynthetic carbon metabolism in transgenic *Arabidopsis thaliana*. *Plant J.* **23**: 759–770.
- Tamura, K., Dudley, J., Nei, M., and Kumar, S.** (2007). MEGA4: Molecular Evolutionary Genetics Analysis (MEGA) software version 4.0. *Mol. Biol. Evol.* **24**: 1596–1599.
- Thompson, J.D., Gibson, T.J., Plewniak, F., Jeanmougin, F., and Higgins, D.G.** (1997). The CLUSTAL\_X Windows interface: Flexible strategies for multiple sequence alignment aided by quality analysis tools. *Nucleic Acids Res.* **25**: 4876–4882.
- Wesley, S.V., et al.** (2001). Construct design for efficient, effective and high-throughput gene silencing in plants. *Plant J.* **27**: 581–590.
- Willats, W.G.T., McCartney, L., Mackie, W., and Knox, J.P.** (2001). Pectin: Cell biology and prospects for functional analysis. *Plant Mol. Biol.* **47**: 9–27.
- Windsor, J.B., Symonds, V.V., Mendenhall, J., and Lloyd, A.M.** (2000). *Arabidopsis* seed coat development: Morphological differentiation of the outer integument. *Plant J.* **22**: 483–493.
- Winter, D., Vinegar, B., Nahal, H., Ammar, R., Wilson, G.V., and Provart, N.J.** (2007). An “electronic fluorescent pictograph” browser

- for exploring and analyzing large-scale biological data sets. *PLoS ONE* **2**: e718.
- Yamada, K., et al.** (2003). Empirical analysis of transcriptional activity in the *Arabidopsis* genome. *Science* **302**: 842–846.
- Zeng, W., Jiang, N., Nadella, R., Killen, T.L., Nadella, V., and Faik, A.** (2010). A glucurono(arabino)xylan synthase complex from wheat contains members of the GT43, GT47, and GT75 families and functions cooperatively. *Plant Physiol.* **154**: 78–97.
- Zhang, Q., and Liu, H.-W.** (2001). Chemical synthesis of UDP- $\beta$ -L-arabinofuranose and its turnover to UDP- $\beta$ -L-arabinopyranose by UDP-galactopyranose mutase. *Bioorg. Med. Chem. Lett.* **11**: 145–149.
- Zhao, G.R., and Liu, J.Y.** (2002). Isolation of a cotton RGP gene: A homolog of reversibly glycosylated polypeptide highly expressed during fiber development. *Biochim. Biophys. Acta* **1574**: 370–374.

**The Interconversion of UDP-Arabinopyranose and UDP-Arabinofuranose Is Indispensable for Plant Development in *Arabidopsis***

Carsten Rautengarten, Berit Ebert, Thomas Herter, Christopher J. Petzold, Tadashi Ishii, Aindrila Mukhopadhyay, Björn Usadel and Henrik Vibe Scheller

*Plant Cell* 2011;23;1373-1390; originally published online April 8, 2011;

DOI 10.1105/tpc.111.083931

This information is current as of February 1, 2012

<b>Supplemental Data</b>	<a href="http://www.plantcell.org/content/suppl/2011/04/04/tpc.111.083931.DC1.html">http://www.plantcell.org/content/suppl/2011/04/04/tpc.111.083931.DC1.html</a>
<b>References</b>	This article cites 62 articles, 27 of which can be accessed free at: <a href="http://www.plantcell.org/content/23/4/1373.full.html#ref-list-1">http://www.plantcell.org/content/23/4/1373.full.html#ref-list-1</a>
<b>Permissions</b>	<a href="https://www.copyright.com/ccc/openurl.do?sid=pd_hw1532298X&amp;issn=1532298X&amp;WT.mc_id=pd_hw1532298X">https://www.copyright.com/ccc/openurl.do?sid=pd_hw1532298X&amp;issn=1532298X&amp;WT.mc_id=pd_hw1532298X</a>
<b>eTOCs</b>	Sign up for eTOCs at: <a href="http://www.plantcell.org/cgi/alerts/ctmain">http://www.plantcell.org/cgi/alerts/ctmain</a>
<b>CiteTrack Alerts</b>	Sign up for CiteTrack Alerts at: <a href="http://www.plantcell.org/cgi/alerts/ctmain">http://www.plantcell.org/cgi/alerts/ctmain</a>
<b>Subscription Information</b>	Subscription Information for <i>The Plant Cell</i> and <i>Plant Physiology</i> is available at: <a href="http://www.aspb.org/publications/subscriptions.cfm">http://www.aspb.org/publications/subscriptions.cfm</a>